REPEATING THERMAL BRIDGES IN CEILINGS AND FLOORS: SIMULATION AND CALCULATION

STAGE 1 FINAL REPORT

10TH JANUARY 2022

ABOUT THIS REPORT

Title: Repeating Thermal Bridges in Ceilings and Floors: Simulation and Calculation – Stage 1 final report

Authors: Alan Green, Steven Beltrame, Georgios Kokogiannakis and Paul Cooper

SBRC SUSTAINABLE BUILDINGS RESEARCH CENTRE | UNIVERSITY OF WOLLONGONG AUSTRALIA

Contact details:

Sustainable Buildings Research Centre (SBRC)

Faculty of Engineering and Information Sciences

University of Wollongong

NSW 2522 Australia

Telephone: +61 (02) 4221 8111

Email: sbrc@uow.edu.au

Web: sbrc.uow.edu.au

Executive Summary

This report outlines Stage 1 of an investigation into thermal bridging by repeating frame members in ceilings and suspended floors. The project is being undertaken by the Sustainable Buildings Research Centre (SBRC) at the University of Wollongong for the Australian Building Codes Board (ABCB).

The investigation has focused on calculation methods specified in the NCC (indirectly, through standards AS 4859.2 and NZS 4214) for calculating the thermal resistance (R-value) of:

- Horizontal ceilings under pitched roofs;
- Suspended floors; and
- Flat, skillion and cathedral-style roofs (with parallel ceiling and roof planes).

And it builds on other projects recently completed by the SBRC, investigating the accuracy of thermal bridge calculation methods in NZS 4214 when applied to horizontal ceilings under pitched roofs [1,2].

Conjugate heat transfer computational fluid dynamics (CFD) simulations and semi-analytical thermal network models have been used to produce reference data, against which the standard calculation methods were compared. Where necessary, modified calculation methods have been developed for improved accuracy.

Key results from each component of the investigation are summarised below, including 11 recommendations (labelled A–K).

HORIZONTAL CEILINGS UNDER PITCHED ROOFS

CFD simulations of horizontal ceilings under pitched roofs in this study have focused on ceilings with ceiling battens and partial 'encapsulation' of frame members by the adjacent ceiling batts (where the batts bulge around the frame members, partially shielding them from radiant and convective heat transfer).

Figure 1 summarises the primary set of results from these simulations. The combined effects of ceiling battens and frame encapsulation were found to bring the R-values of steel-framed ceilings into closer alignment with equivalent timber-framed assemblies, as compared to the results from previous studies where these features were not modelled.

The standard NZS 4214 calculation method produced significant errors in several cases, particularly those involving unmitigated steel thermal bridges and higher batt R-values.

A modified version of the method was developed and calibrated using the CFD results from this study. It is identical to the modified method developed previously for the ABCB [1], except that the pseudo air-space R-value (R_{pa}) is varied as a function of the ceiling construction details.

An updated set of deemed to satisfy (DTS) thermal bridge mitigation measures were developed using the modified calculation method (Table 1).
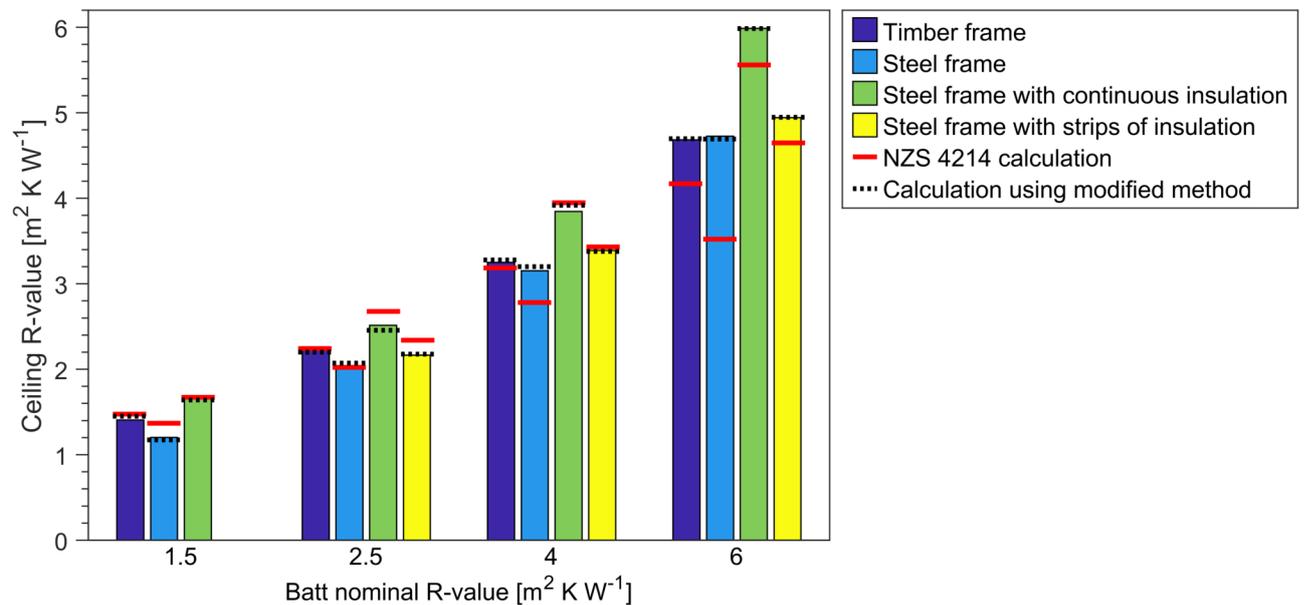

Figure 1: Ceiling R-values (not including 'film resistances') determined from CFD simulations of Cases 1–15, and compared to values calculated using the NZS 4214 method and a modified method developed in this study and calibrated using the CFD results.

Recommendations:

A. The CFD simulations presented here have demonstrated once again that the standard NZS 4214 thermal bridge calculation method should not be used to calculate the R-value of horizontal ceilings under pitched roofs when: (i) the roof space is not included in the calculation, and (ii) the thermal bridging is relatively severe (such as that caused by unmitigated steel bridges). Our previous investigations have also demonstrated that alternative one-dimensional thermal bridge calculation methods used in other jurisdictions suffer from similar levels of inaccuracy when applied to such ceilings, so they do not offer a solution to this problem. We recommend that a modified calculation

method like that developed here be used in such cases. In Stage 2 of this project we will develop a more generally applicable calculation method for this purpose.

B. The thermal bridge mitigation measures outlined in Table 1 represent the minimum level of mitigation needed to meet the targets specified by the ABCB (i.e. to bring steel-framed ceilings to within 95 or 90 % of timber-framed R-values, depending on the level of insulation). We recommend that the practicability of such minor mitigation measures be considered, and that, if appropriate, these mitigation measures are either omitted altogether from the NCC or updated to meet alternative performance targets.

C. We recommend that, if the option to mitigate thermal bridges using strips of insulation installed over frame members is offered in the NCC, a requirement is included that the strips form a continuous layer of insulation with other insulation in the assembly. Otherwise, strips of insulation could be installed over frame members that protrude above ceiling batts (e.g. 90 mm frame members with R1.5 batts), leaving gaps in the thermal control layer and failing to mitigate thermal bridging effectively.

D. We recommend that the standard NZS 4214 be updated with a less ambiguous explanation of how the boundaries of thermally bridged layers should be defined, in line with the original work by Trethowen [3,4].

E. We recommend that further work be carried out to develop a generally applicable modified version of the NZS 4214 thermal bridge calculation method for application to building assemblies like the ceilings investigated here; and that the modified calculation method be included in NZS 4214. Without such a method being available to NCC practitioners, they are unable to accurately calculate the R-value of some types of building assemblies when attempting to meet minimum R-values specified in the NCC. Stage 2 of this project will build towards this goal.

F. We recommend that the treatment of thermal bridges in NatHERS software be reviewed, and that the methods be updated to address the issues demonstrated in this report if necessary.

Table 1: Updated minimum mitigation measures for Tables 13.2.3v and J3D7v of NCC 2022. These values represent the minimum level of mitigation needed to bring archetypal steel-framed ceilings to within either 95% or 90% of the R-value of corresponding archetypal timber-framed ceilings, as described in Section 2.1.

Minimum R-value from Tables 13.2.3a to 13.2.3i, and Table 13.2.3s if applicable	Option 1 - Increase insulation between ceiling framing to specified minimum R-value	Option 2 - Add insulation strips with specified minimum R-value above or below the ceiling framing	Option 3 - Add a layer of continuous insulation with specified minimum R-value above or below the ceiling framing
1.5	1.64	0.45	0.06
2.0	2.07	0.40	0.03
2.5	2.52	0.32	0.01
3.0			
3.5			
4.0			
4.5		No mitigation required	
5.0			
5.5			
6.0			

SUSPENDED FLOORS

CFD simulations of carpeted timber- and steel-framed suspended floor assemblies were used to investigate whether the same types of issues apply to them when using the standard NZS 4214 thermal bridge calculation method, and to assess the nominal R-values specified for subfloor spaces in Table S39C2a of the NCC 2022 draft. In cases where the thickness of floor batts was less then the floor joist height, they could be installed either 'high' (i.e. flush with the top of the joist) or 'low' (i.e. flush with the bottom of the joist), and both alternatives were simulated.

Figure 2 presents the primary results from this investigation. Floors with unmitigated steel thermal bridges were found to have R-values equal to 64–81 % of the corresponding timber-framed floor R-value.

The impact of thermal bridge mitigation measures in the draft NCC 2022 DTS provisions varied. Continuous insulation installed below the floor successfully brought the R-value of steel-framed floors to within 95% of the corresponding timber-framed floor R-values when the floor batts were R1 or R2, but did not meet the target thresholds in cases with R3 or R4 batts.

Strips of insulation modelled on the underside of the joists were less effective, and failed to meet the target R-values in all cases simulated.

Timber- and steel-framed floors were also simulated with foil-faced R0.11 foam wall wrap draped over their joists, instead of bulk insulation. These floors were found to have R-values of 0.94 and 0.71 m^2 K W^{-1}, respectively, and the foil facing on the underside of the foam insulation added an additional 0.7–1.0 m^2 K W^{-1} to the effective R-value of the subfloor space. It should be noted that compression of the foam wall wrap was not modelled in this study.
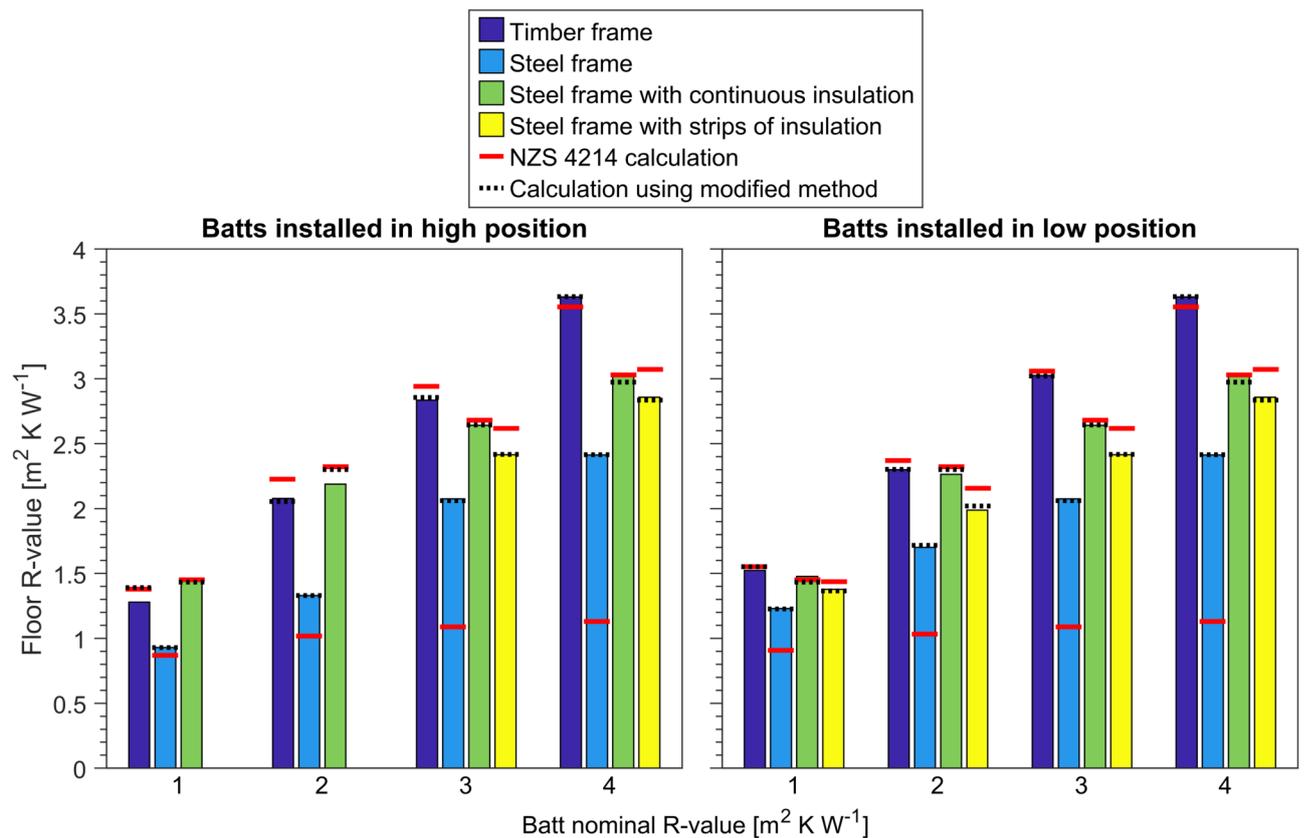

Figure 2: R-values of floor assemblies (not including 'film resistances') from CFD simulations of Cases 1–23, compared to standard NZS 4214 calculations and calculations using the modified method developed here. The left- and right-hand graphs display results from cases the bulk floor insulation is installed flush with the top and bottom surfaces of the floor joists, respectively. Results from cases where the bulk insulation height equals the joist height are included in both graphs.

The standard NZS 4214 calculation method introduced significant errors when applied to steel-framed suspended floors with no thermal bridge mitigation, which aligns with results from previous studies focused on ceiling assemblies with similar construction details. In general, the NZS 4214 method was relatively accurate in other cases, but significant errors did arise in some cases due to particularly two-dimensional heat flow (e.g. where the timber frame protrudes far

below the underside of floor batts, or where heat was able to partially bypass strips of insulation installed on the underside of joists).

The same type of modified calculation method that was applied to horizontal ceilings under pitched roofs in this study was calibrated and applied to suspended floors, which typically improved the accuracy of R-value predictions significantly (Figure 2).

The nominal R-values specified for subfloor spaces in Table S39C2a of the NCC 2022 draft (and similar values in Table 16 of AS 4859.2) were much lower than those determined in this study through CFD. The NCC specifies a single value of $0.417 \ m^2 \ K \ W^{-1}$ that applies to all subfloors that were simulated, whereas CFD predicted values 4 times higher for most cases, and between 7 and 11 times higher in cases with low-emittance surfaces on the underside of the floor assembly. A large part of this discrepancy is likely to be due to the differences in the assumptions used in each case. For example, the soil thermal conductivity, subfloor wall thermal resistance, subfloor wall height, thermal emittance of surfaces bounding the subfloor space, and subfloor ventilation rate can all have large impacts on subfloor space effective R-value, but are accounted for in Table S39C2a.

Recommendations:

G. When calculating the R-value of suspended floors separately from the subfloor space (as required under the draft NCC 2022 Housing Provisions), and the thermal bridging is severe (e.g. unmitigated metal frame members penetrating floor batts), the standard NZS 4214 calculation method should not be used. A modified calculation method can be applied to such floors. The method developed here produces accurate R-value estimates for suspended floors with the same construction details as those simulated here, and Stage 2 of this project is intended to produce a more generally applicable calculation method.

H. When calculating the R-value of suspended floors including the subfloor space (as required under the draft NCC 2022 Volume 1), the standard NZS 4214 calculation method is valid. However:

   a. The accuracy of the method in such cases will depend on the nominal R-value assigned to the subfloor space; and

   b. Instructions in NZS 4214 are currently ambiguous as to whether the subfloor space should be included in the 'bridged layer' in such calculations.

These issues are addressed in Recommendations I and D, respectively.

I. We recommend that, if Volume 1 of the NCC continues to require users to apply nominal R-values to subfloor spaces, those values (currently contained in Table S39C2a) be reviewed, and if appropriate, updated to account for factors such as the thermal emittance of surfaces bounding the subfloor space and the thermal resistance and height of subfloor walls. The review should also address inconsistencies between the subfloor space R-values specified in the NCC and those specified in Table 16 of AS 4859.2.

FLAT, SKILLION AND CATHEDRAL ROOFS

Flat, skillion and cathedral-style roofs (i.e. those with parallel ceiling and roof planes) are treated separately from horizontal ceilings under pitched roofs within the NCC. The thermal performance of such roofs is assessed using a single R-value, rather than separating the ceiling assembly from a roof space above.

An advantage of this approach is that there is no need to calculate the R-value of a ceiling assembly separately from an adjacent roof space, so the issues that cause the NZS 4214 thermal bridge calculation method to be inaccurate when applied to other ceilings should theoretically not apply. However, the disadvantage of characterising flat/skillion/cathedral roofs using one R-value is that any ventilated cavities therein are modelled using the relatively simplistic, and arguably unrealistic, guidelines in AS 4859.2.

Previous investigations by the SBRC, and others, have demonstrated how ventilated cavities can increase the effective thermal resistance of building assemblies under realistic conditions. However, the procedures described in AS 4859.2 (which are prescribed in the NCC) are based on an assumption that ventilation of air-filled cavities must degrade the assembly's R-value.

To demonstrate the magnitude of error that this issue can introduce for flat/skillion/cathedral roofs, a thermal network model was developed and coupled with a flow network model to predict cavity ventilation rates. Application of the models to a case study skillion roof under a variety of boundary conditions produced the results shown in Figure 3.

Clearly, the assumed impacts of cavity ventilation in AS 4859.2 are not realistic in these sets of steady-state scenarios, and lead to a significant underestimation of the skillion roof R-value. This analysis could be extended quantify the accumulated impact of such inaccuracy over a year of operation in various locations, and with various roof constructions.
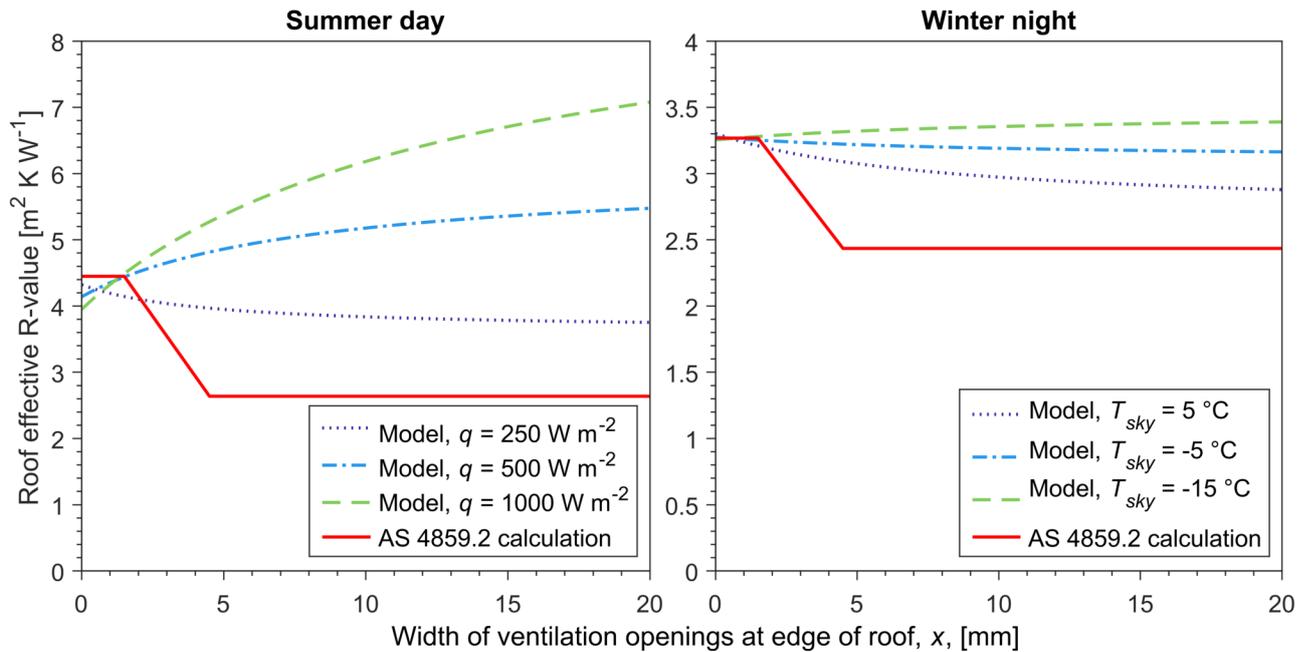
Figure 3: Comparison of skillion roof R-values determined using a thermal network model against the values calculated according to AS 4859.2. Results are presented over a range of ventilation opening sizes (x), and under several different steady-state conditions, including: (left) summer days with solar various solar heat fluxes (q) incident on the roof top surface; and (right) winter nights with various sky radiant temperatures (T_{sky}). Note that the two graphs have different vertical scales.

Recommendations:

J. The issues that arise when applying the NZS 4214 thermal bridge calculation method to ceilings or suspended floors and not including the adjacent air space in the calculation (discussed in Sections 2 and 3), do not necessarily apply to typical flat/skillion/cathedral roofs. However, if a cavity in the roof is classified as 'well' or 'slightly' ventilated under AS 4859.2, NCC practitioners are forced to calculate the roof R-value omitting that cavity and any other material layers on one side of it. This can give rise to situations where thermal bridges are exposed to an air space that is omitted from the calculation, in which case a modified version of NZS 4214 is likely to be needed. We recommend that the treatment of ventilated cavities in AS 4859.2 be reviewed and improved (see also Recommendation K, which is related).

K. The treatment of ventilated cavities in AS 4859.2 is likely to introduce significant errors in R-value calculations for flat/skillion/cathedral roofs that qualify as 'slightly' or 'well' ventilated under the standard. We recommend that the methods prescribed for ventilated cavities in AS 4859.2 be revised to more accurately represent the

accumulated annual impact of such cavities when exposed to realistic boundary conditions (including separate outdoor radiant and convective heat transfer).

Table of contents

List of abbreviations

ABCB   Australian Building Codes Board

AIRAH   Australian Institute of Refrigeration, Air Conditioning and Heating

ASHRAE   American Society of Heating, Refrigerating and Air-Conditioning Engineers

CFD   Computational fluid dynamics

DTS   Deemed to satisfy

NASH   National Association of Steel-Framed Housing

NatHERS   Nationwide House Energy Rating Scheme

NCC   National Construction Code

R-value   Effective thermal resistance [m^2 K W^{-1}]

SBRC   Sustainable Buildings Research Centre

1 Introduction

This is the final report from Stage 1 of an ongoing investigation into thermal bridging by repeating frame members in ceiling and suspended floor assemblies, conducted by the Sustainable Buildings Research Centre (SBRC) at the University of Wollongong for the Australian Building Codes Board (ABCB).

1.1 BACKGROUND

The draft National Construction Code (NCC) 2022 energy efficiency provisions include explicit requirements for building designers to account for thermal bridging effects via one of the following verification methods.

- **Prescriptive solutions:** Meet the deemed to satisfy (DTS) minimum requirements for the building envelope, which are specified in terms of:
    - Minimum insulation batt R-values required in each assembly, determined based on an assumed level of thermal bridging equivalent to that caused by typical timber frames; and
    - Additional mitigation measures that must be taken in steel-framed assemblies.
- **Calculation:** Account for thermal bridges when calculating the thermal resistance (R-value) of building envelope assemblies. NCC practitioners are directed to follow methods outlined in AS/NZS 4859.2 [5], which prescribes the NZS 4214 isothermal planes calculation method [6] for estimation of thermal bridging effects.
- **Simulation:** Verify the compliance of proposed buildings through NatHERS building performance simulations, or other similar simulations, which include the effects of thermal bridging in envelope assemblies.

Such explicit requirements for practitioners to account for thermal bridging effects constitute a significant change in the NCC (introduced for Class 2–9 buildings in 2019, and proposed to be introduced for Class 1 buildings and Class 10 buildings with a conditioned space in 2022).

The thermophysical processes involved in thermal bridging can be very complex, involving transient conductive, convective and radiant heat transfer through complicated three-dimensional geometries. Given this complexity, and the need for practical and generalisable provisions within the NCC, all

three of the methods for estimating thermal bridging effects outlined above necessarily rely on simplified models of reality. The NZS 4214 calculation method represents building assemblies as one-dimensional resistance networks; NatHERS building performance simulations estimate thermal bridging effects using the NZS 4214 method or similar one-dimensional calculation methods, depending on the type of thermal bridge [7]; and prescriptive DTS solutions are developed using NatHERS simulations and NZS 4214 calculations [8].

Recent investigations by the SBRC [1,2,9], and by others [10], have demonstrated that the NZS 4214 method can produce inaccurate results when applied inappropriately. The foundational work on which the method was based [3,4] validated it against experimental results for a range of wall and roof assemblies and developed a detailed set of guidelines for its implementation. However, those guidelines have not been specified completely within the current version of the standard, and limits to the validity of the method have not yet been comprehensively established [1].
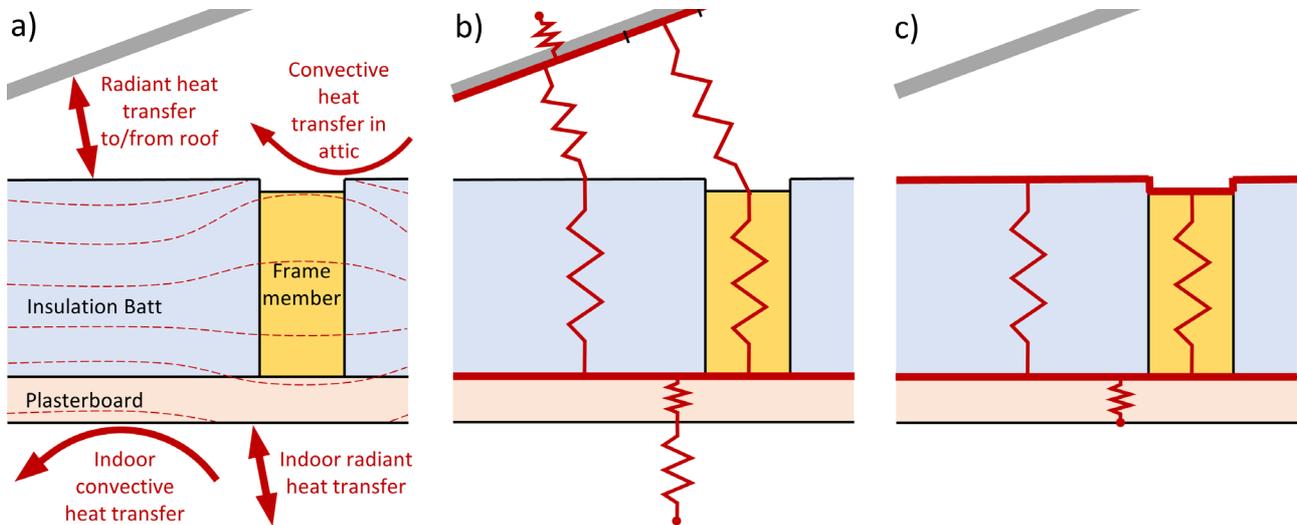
In particular, a recent project completed by the SBRC for the ABCB [1], and an extension on that project completed by the SBRC for NASH [2], have demonstrated limitations in how the NZS 4214 method should be applied to horizontal ceiling assemblies under pitched roofs. Under the NCC, the R-values of such ceilings need to be determined separately from the roof space and roof, because:

- DTS provisions for ceilings are developed in this way;
- Minimum R-values to be met via calculations are also specified on this basis; and
- NatHERS software needs to calculate the R-value of the ceiling assembly so that it can be modelled between the thermal zones formed by the indoor space and roof space.

This approach has a significant advantage over the alternative (where ceilings, roof spaces and roofs would be combined and represented by a single R-value), in that the transient thermal performance of the roof space can be accurately modelled for each climate and roof design. However, we have shown that the standard NZS 4214 method can severely over-predict the thermal bridging impact of steel frame members when applied to ceiling assemblies in this way [1].

Figure 4 illustrates the issue schematically. When the NZS 4214 method is applied to an entire roof/ceiling assembly (Figure 4b), the roof space should be included in the 'thermally bridged layer', thereby allowing the top surfaces of ceiling batts and frame members to reach different temperatures. However, when the NZS 4214 method is applied to the ceiling assembly only (Figure 4c), the calculation assumes that the top surfaces of ceiling batts and frame members are at an equal

temperature. This assumption can influence the predicted heat transfer rate through the thermal bridges (i.e. frame members) significantly.

Figure 4: Schematic diagrams of heat transfer through a horizontal ceiling under a pitched roof: (a) primary heat transfer pathways and approximate isotherms (red dashed lines); (b) application of the NZS 4214 method to the entire ceiling and roof assembly; and (c) application of the NZS 4214 method to the ceiling assembly only (as required within the NCC).

It should be noted that these issues and limitations are not unique to the NZS 4214 method. Similar one-dimensional thermal bridge calculation methods used in other jurisdictions (e.g. the ISO 6946 method [11], Gorgolewski method [12,13], and modified zone method [14]) also produce inaccurate results when applied to certain types of building assembly, or when implemented incorrectly.

In our recent study [1], we developed a modified version of the NZS 4214 method that produces accurate R-value estimates for a range of steel-framed ceilings covered in that investigation. The method was then compared to a broader range of cases in a subsequent investigation [2]. Amongst other changes, this second study included cases with:

- Ceiling battens installed between the ceiling joists/truss bottom chords and plasterboard ceiling lining; and
- Partial or complete 'encapsulation' of frame members by adjacent ceiling batts, where the insulation bulges above the frame member and (partially or completely) insulates it from the roof space above.

It was found that the modified NZS 4214 method is not accurate for all cases (in particular, it was not more accurate than the standard NZS 4214 method when applied to steel-framed ceilings with

battens). Moreover, the significant effects of details such as ceiling battens and frame encapsulation on the overall ceiling R-value were demonstrated.

The current project has been commissioned by the ABCB to investigate this and several related issues that have arisen through the NCC 2022 public comment process. Further details are provided in the following section.

1.2 PROJECT OUTLINE

The current project is divided into two stages. Stage 1 of the project involves simulations and analysis of timber and steel thermal bridges in:

- Horizontal ceilings under pitched roofs;
- Suspended floors; and
- Flat, skillion and cathedral roofs.

Stage 2 will extend on that analysis to develop a calculation method for estimation of the thermal resistance of horizontal ceilings under pitched roofs.

1.2.1 Aims and Objectives

The project has four primary aims, as follows.

1. Produce an updated version of Table 13.2.3v (which outlines DTS thermal bridge mitigation measures for horizontal steel-framed ceilings under pitched roofs in the draft NCC 2022 Housing Provisions, and is equivalent to Table J3D7v in Volume 1), based on an accurate assessment of timber- and steel-framed ceiling R-values and an updated set of modelling assumptions. The new modelling assumptions include:
   a. Ceiling battens;
   b. A realistic level of frame 'encapsulation';
   c. Steel frame base metal thickness of 0.75 mm; and
   d. Timber thermal conductivity of $0.12 \text{ W m}^{-1} \text{ K}^{-1}$.
2. Evaluate the accuracy of the NZS 4214 thermal bridge calculation method when applied to suspended floor assemblies, as well as the nominal R-values for subfloor spaces in Table S39C2a in the draft NCC 2022 provisions, and propose a correction to the NZS 4214 method for suspended floors if one is needed.

3. Provide a concise review of limitations and possible improvements to how the R-values of flat, skillion and cathedral roofs are assessed under the NCC.

4. Develop a calculation method to estimate the R-value of thermally bridged horizontal ceilings under pitched roofs. The method is to be suitable for possible implementation in NatHERS software, and other similar building performance simulation software.

The first three of these aims are being addressed in Stage 1 of the project, and the fourth aim will be addressed in Stage 2.

2 Horizontal Ceilings under Pitched Roofs

The first investigation in this project was focused on thermal bridging in horizontal ceilings under pitched roofs. Bulk insulation in the form of ceiling batts is typically installed between the roof truss bottom chords or ceiling joists, creating thermal bridges wherever those frame members penetrate the insulation layer.

This work builds on findings from our two recent projects [1,2], and feedback provided to the ABCB through the NCC public comment processes, with an aim to provide an updated table of DTS thermal bridge mitigation measures for possible inclusion in the NCC in 2022.

2.1 PROBLEM STATEMENT

The DTS thermal bridge mitigation measures specified for horizontal steel-framed ceilings under pitched roofs in Tables 13.2.3v and J3D7v of the draft NCC 2022 provisions are based on an analytical comparison between 'typical' timber- and steel-framed ceiling assemblies. The mitigation measures are specified such that they bring the calculated R-value of steel-framed ceilings to:

- At least 95 % of the thermal resistance of an equivalent timber-framed ceiling, in cases with ceiling batt R-values of up to 3 W m^{-1} K^{-1}, and
- At least 90 % of the thermal resistance of an equivalent timber-framed ceiling, in cases with ceiling batt R-values of more than 3 W m^{-1} K^{-1}.

Two challenges in developing such mitigation measures are:

1. In defining 'typical' timber- and steel-framed assemblies; and
2. In calculating accurate ceiling assembly R-values to compare (due to the inaccuracy of the NZS 4214 method, and other similar methods, when applied to such assemblies [1]).

The first of these challenges has been addressed by the ABCB through the NCC public comment process, and through consultation with the Energy Efficiency Technical Working Group Thermal Bridging Subgroup. Feedback from those processes has been synthesised to produce the timber- and steel-framed ceiling assemblies investigated here.

The SBRC has addressed the second challenge listed above in recent projects [1,2] by using conjugate heat transfer CFD simulations to provide reference data on the R-value of thermally bridged ceilings.

Such R-values can be used to perform direct comparisons between timber- and steel-framed ceilings, and to validate improved calculation methods.

This investigation has been conducted to produce an updated set of thermal bridge mitigation measures for horizontal steel-framed ceilings under pitched roofs, similar to Tables 13.2.3v and J3D7v, and based on the updated 'typical' timber- and steel-framed ceilings.

2.2 METHODOLOGY

Three-dimensional, steady-state conjugate heat transfer CFD simulations were run to quantify the R-value of timber- and steel-framed ceilings. This technique models three-dimensional thermal conduction through the ceiling assembly, as well as air flow, convective heat transfer and radiant heat transfer through air-filled zones (e.g. the roof space above the ceiling and any cavities formed within the ceiling assembly). More detail on the CFD methods and settings is provided in Appendix A.

The scope of the current project did not allow for every case in the updated version of Tables 13.2.3v and J3D7v to be simulated using CFD, especially given that iterative simulations would need be run in order to arrive at the minimum level of mitigation required in each scenario. Instead, a fixed set of cases was simulated and used to develop a calculation method for accurate prediction of thermal bridging effects in ceilings. The calculation method was then used to generate an updated table of DTS mitigation measures.

When applying the NZS 4214 calculation method, or our modified version of that method, to ceiling assemblies, the following approach was taken.

- The guidelines developed by Trethowen [3] were followed where relevant.
- When applied to ceilings with ceiling battens, four heat transfer pathways were identified:
    i. One through the ceiling batts;
    ii. One through the ceiling joists and cavity formed between the joists and plasterboard;
    iii. One through the battens and batts; and
    iv. One through the battens and joists.
- The effective R-values of any cavities formed within the ceiling assembly (e.g. between joists and plasterboard) were determined using methods specified in Appendix D of ISO 6946 [11].
- Resistances of 0.03 m^2 K W^{-1} were included between any two rigid materials in contact.

2.3 CASES INVESTIGATED

2.3.1 Ceiling Assemblies

Table 2 outlines the set of cases that were simulated. It covers timber- and steel-framed ceiling assemblies, with a range of insulation thicknesses, and including steel-framed cases with and without additional thermal bridge mitigation measures.

Table 2: Overview of ceiling assemblies simulated.

| Case | Frame | | | Ceiling battens | | | Insulation | | Mitigation measure[3] |
	Material	Dimensions[1] [mm]	Frame factor[2] [%]	Material	Dimensions[1] [mm]	Spacing [mm]	R-value [m² K W⁻¹]	Thickness [mm]	
1	steel	90×40×0.75	6	steel	20×60×0.42	600	1.5	72	none
2	steel	90×40×0.75	6	steel	20×60×0.42	600	2.5	120	none
3	steel	90×40×0.75	6	steel	20×60×0.42	600	4	192	none
4	steel	90×40×0.75	6	steel	20×60×0.42	600	6	288	none
5	steel	90×40×0.75	6	steel	20×60×0.42	600	2.5	120	R0.51 strips on frame
6	steel	90×40×0.75	6	steel	20×60×0.42	600	4	192	R0.51 strips on frame
7	steel	90×40×0.75	6	steel	20×60×0.42	600	6	288	R0.51 strips on frame
8	steel	90×40×0.75	6	steel	20×60×0.42	600	1.5	72	R0.26 continuous insulation over frame
9	steel	90×40×0.75	6	steel	20×60×0.42	600	2.5	120	R0.38 continuous insulation over frame
10	steel	90×40×0.75	6	steel	20×60×0.42	600	4	192	R0.38 continuous insulation over frame
11	steel	90×40×0.75	6	steel	20×60×0.42	600	6	288	R0.51 continuous insulation over frame
12	timber	90×35	8.4	steel	20×60×0.42	600	1.5	72	none
13	timber	90×35	8.4	steel	20×60×0.42	600	2.5	120	none
14	timber	90×35	8.4	steel	20×60×0.42	600	4	192	none
15	timber	90×35	8.4	steel	20×60×0.42	600	6	288	none
16 [4]	steel	90×40×0.75	6	steel	20×60×0.42	600	2.5	120	R0.38 continuous insulation under frame
17 [5]	timber	90×35	5.25	steel	20×60×0.42	600	6	288	none
18 [6]	timber	90×35	8.4	n/a	n/a	n/a	2.5	120	none

[1] *Frame member and batten dimensions are expressed as: height × width × base metal thickness (where relevant).*

[2] *Frame factor equals the fraction of the ceiling projected area that is occupied by frame members.*
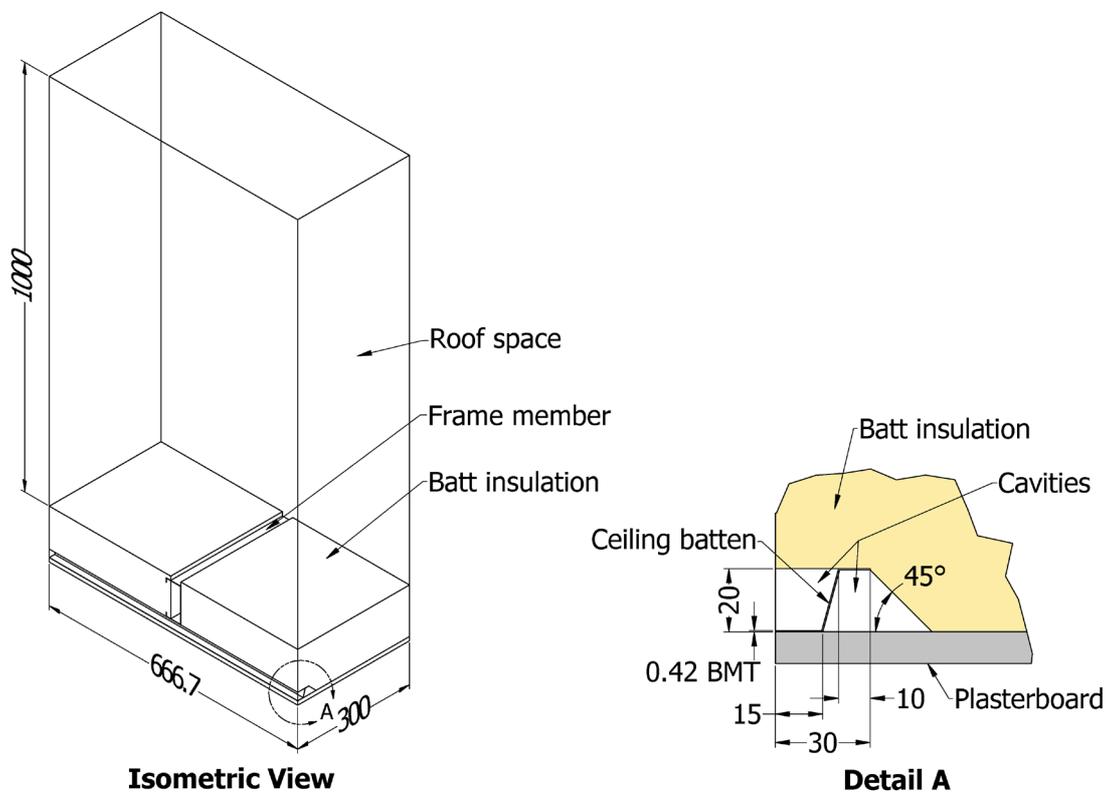
[3] *The simulated thermal bridge mitigation measures were taken from the draft NCC 2022 Housing Provisions, and involve either installing strips of insulation over the ceiling frame members or installing a continuous insulation layer above the ceiling frame. Results from the CFD study were used to develop a modified calculation method, which was then used to produce updated minimum R-values for such insulation strips or continuous insulation, for possible inclusion in NCC 2022.*

[4] *One case was run with continuous insulation installed below the frame (directly above the plasterboard and below the ceiling battens), rather than above, to validate R-value calculations of such assemblies.*

[5] *One timber-framed case was simulated with the same effective frame spacing as the steel-framed cases and with R6 batt insulation, to assist in the analysis of Cases 4 and 15.*

[6] *One case was simulated with timber-framed ceiling and no ceiling battens, to allow the influence of ceiling battens to be better understood.*

Each ceiling assembly was modelled in three dimensions, so that the three-dimensional heat flow near the intersection of frame members and ceiling battens could be simulated accurately. The computational domain defined for each simulation contained one frame member intersecting one batten, except that only half of the batten was modelled, and a 'symmetry' boundary condition was used to model the influence of the other half of the batten (Figure 5). This approach, in which only part of the ceiling and roof space is simulated, was compared to two-dimensional simulations of entire roof/ceiling assemblies in our previous project [2], and was shown to produce equivalent ceiling R-values when boundary conditions were set correctly.

Isometric View   **Detail A**

Figure 5: Example of the type of three-dimensional computational domain developed for the simulations of horizontal ceilings under pitched roofs. Only half of the batten was included in the domain, and a 'symmetry' boundary condition was applied to the plane that cuts the batten in half. Dimensions are expressed in mm.

Partial encapsulation of frame members by the ceiling batts was modelled in all cases, as illustrated in Figure 6. The degree of encapsulation assumed in each case was based on physical tests in our previous project [2] and an assumption that the batt width is 20 mm less than the frame centre-to-centre spacing in all cases. While the nominal batt width did not change, the width of the gap between adjacent batts (x in Figure 6) was reduced as batt thickness increased, to account for the effects of

insulation fibres protruding into the gap, uneven batt edges and batt edges that are not exactly vertical. Timer- and steel-framed cases were modelled with equal gap widths.
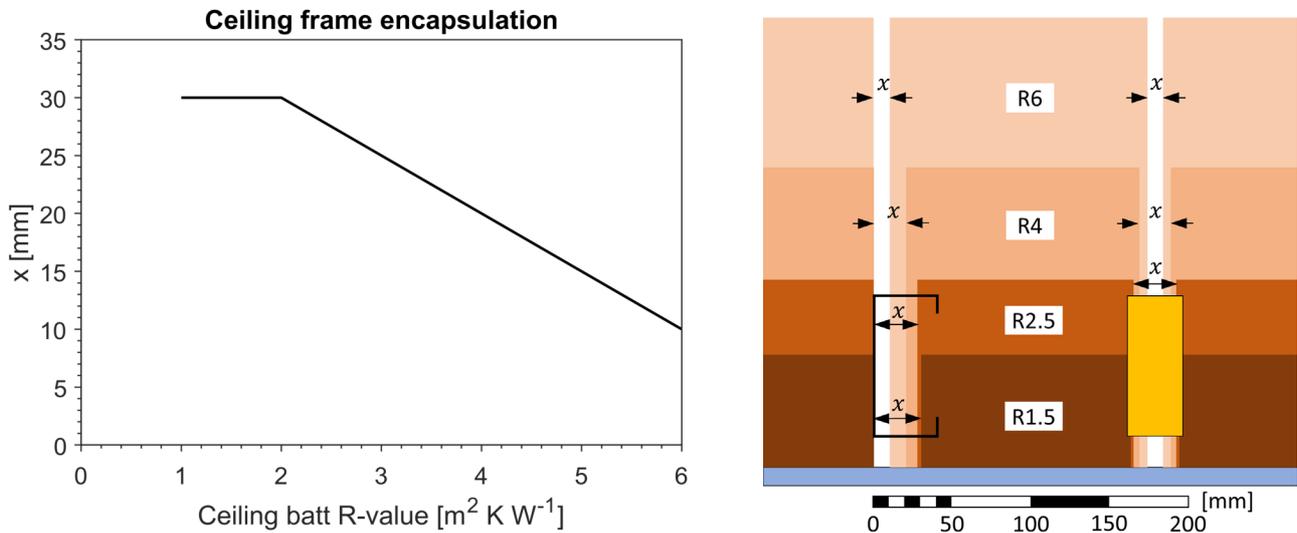

Figure 6: Levels of frame encapsulation modelled in cases with different ceiling batt R-values: (left) the function used to determine the gap between adjacent batts (x); and (right) cross-sections illustrating how batts of different R-values were assumed to fit around steel and timber frame members (note that the frame members are held 20 mm above the plasterboard by perpendicular battens, which are not intersected by these cross-sections).

2.3.2 Material Properties

Material properties applied in the CFD simulations are summarised in Table 3. They are identical to those used in the recent projects completed for the ABCB [1] and NASH [2], except for the following.

- The thermal conductivity of timber is set to 0.12 W m^{-1} K^{-1}, rather than 0.1 W m^{-1} K^{-1}. A review of relevant literature and published data in our recent project [2] revealed that the thermal conductivity of timber can vary widely depending on the timber species, moisture content, grain orientation relative to heat flow, and unique characteristics of each sample. The value of 0.12 W m^{-1} K^{-1} is specified for softwoods (e.g. pine) at 12 % moisture content in NZS 4214 [6].

- The thermal conductivity of mineral wool decreases in regions where ceiling batts are compressed above battens, according to the function shown in Figure 7.

- The thermal emittance of steel varies depending on its orientation (since the level of dust cover is assumed to be more for upward-facing surfaces); this assumption was taken in the NASH study, but not the ABCB study.

Table 3: Thermal material properties applied in simulations of ceiling assemblies.

Material	Thermal conductivity [W m⁻¹ K⁻¹]	Thermal emittance
Timber	0.12	0.9
Steel	47.5	0.23 or 0.28 [1]
Plasterboard	0.17	0.9
Mineral wool ceiling batts	0.048 [2]	0.9
Continuous insulation and strips of insulation used for thermal bridge mitigation	0.035	0.9

[1] *Based on a value of 0.23 for bright galvanized steel and increased by 0.05 for upward-facing surfaces to account for light dust cover* [15].

[2] *The thermal conductivity of ceiling batts decreases as illustrated in Figure 7 in regions where the batts are compressed above a ceiling batten.*

Figure 7: Variation of ceiling batt thermal conductivity with density, where the density increases in localised regions of batt compression above ceiling battens. The function in this table is based on material data published in the AIRAH Technical Handbook [15].

Contact resistances of 0.03 m² K W⁻¹ were included at the interfaces between any two rigid materials in contact (i.e. between battens and plasterboard, between battens and joists, and between joists and plasterboard).

2.3.3 Boundary Conditions

The scope of this study only allowed one set of boundary conditions to be investigated. While the boundary conditions (e.g. outdoor air temperature, solar heat flux, etc.) can have a large impact on the effective R-value of a roof space, the R-value of the ceiling assembly does not change significantly.

The set of boundary conditions applied in this study are outlined in Table 4. They are based on simulations of entire roof/ceiling assemblies operating under summer daytime conditions in the original ABCB study [1], including an outdoor air temperature of 35 °C, absorbed solar heat flux on the roof top surface of 500 W m^{-2}, and roof space ventilation rate of 13.2 air changes per hour.

Table 4: Ceiling simulation boundary conditions.

Parameter	Value
Indoor temperature	25 °C
Indoor 'film resistance'	0.12 m^2 K W^{-1}
Roof space air temperature	37.85 °C
Roof space reference air speed	0.175 m s^{-1}
Roof mean radiant temperature ('viewed' from top of ceiling assembly)	49.85 °C
Roof bottom surface thermal emittance ('viewed' from top of ceiling assembly)	0.03

2.4 RESULTS

Ceiling R-values determined from the CFD results are summarised in Table 5, and R-values from the primary set of simulations (Cases 1–15) are presented in Figure 8, where they are compared to values calculated using the standard NZS 4214 method and a modified calculation method developed here.

2.4.1 Ceiling Thermal Resistance

The R-values of steel-framed ceilings were typically lower than those of equivalent timber-framed ceilings. For example, in cases with R1.5–R4 insulation, the steel-framed ceiling R-values equalled 85–97 % of those from corresponding timber-framed cases.

However, in cases with R6 insulation (i.e. Cases 4 and 15), the steel-framed ceiling R-value was slightly higher than that of the timber-framed ceiling (i.e. equal to 100.9 % of the timber-framed value). The primary cause for this appears to be the difference in frame factor between timber- and steel-framed cases, as demonstrated by Case 17, which has a timber frame but an equal effective frame spacing to the steel-framed cases and exhibits a significantly higher ceiling R-value. Thus, while steel frame members do form thermal bridges that are more severe than those formed by timber, the combination of: (i) lower frame factors, (ii) increasing levels of frame encapsulation as the ceiling batt thickness increases, and (iii) battens forming something of a thermal break below the ceiling

frame, the R-value of steel-framed ceilings can exceed that of timber-framed ceilings when the nominal batt R-value exceeds a value close to 6 m^2 K W^{-1}.

Table 5: Ceiling R-values (not including 'film resistances') determined from each CFD simulation.

Case	Frame	Frame factor [%]	Ceiling battens	Insulation R-value [m^2 K W^{-1}]	Mitigation measure	Ceiling R-value [m^2 K W^{-1}]	Ratio of ceiling R-value to that of corresponding timber-framed case [%]
1	steel	6	steel	1.5	none	1.2015	85.35
2	steel	6	steel	2.5	none	2.0353	90.00
3	steel	6	steel	4	none	3.1521	97.02
4	steel	6	steel	6	none	4.7250	100.90
5	steel	6	steel	2.5	R0.51 strips on frame	2.1651	95.75
6	steel	6	steel	4	R0.51 strips on frame	3.3893	104.32
7	steel	6	steel	6	R0.51 strips on frame	4.9432	105.56
8	steel	6	steel	1.5	R0.26 continuous insulation over frame	1.5585	110.71
9	steel	6	steel	2.5	R0.38 continuous insulation over frame	2.5128	111.12
10	steel	6	steel	4	R0.38 continuous insulation over frame	3.8469	118.40
11	steel	6	steel	6	R0.51 continuous insulation over frame	5.9892	127.90
12	timber	8.4	steel	1.5	none	1.4077	100.00
13	timber	8.4	steel	2.5	none	2.2613	100.00
14	timber	8.4	steel	4	none	3.2491	100.00
15	timber	8.4	steel	6	none	4.6828	100.00
16	steel	6	steel	2.5	R0.38 continuous insulation under frame	2.4461	108.17
17	timber	5.25	steel	6	none	5.0498	n/a
18	timber	8.4	none	2.5	none	2.1889	n/a

Both mitigation measures simulated proved to be effective in raising the steel-framed ceiling R-value above 95 % of corresponding timber-framed ceilings. However, in most cases the quantity of additional insulation (in the form of strips or continuous insulation) specified in the draft NCC 2022 Housing Provisions was significantly higher than it needed to be, as demonstrated by the fact that most of the 'mitigated' steel-framed ceilings had R-values higher than the timber-framed equivalents.

2.4.2 Accuracy of Calculation Methods

While the standard NZS 4214 calculation method was relatively accurate in several cases, it was inaccurate by as much as 25 % in other cases (Figure 8). Typically, this method was least accurate in

cases with a steel-framed ceiling and no mitigation measures, and in cases with thicker batts (and therefore also higher degrees of encapsulation).
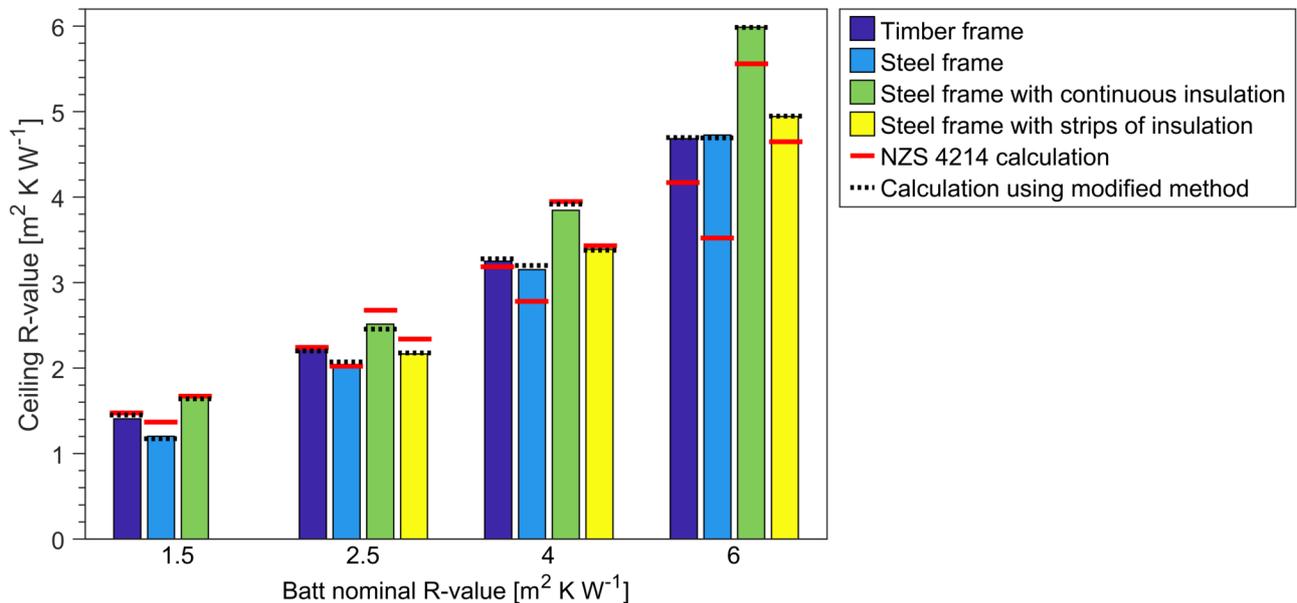

Figure 8: Ceiling R-values (not including 'film resistances') determined from CFD simulations of Cases 1–15, and compared to values calculated using: (i) the NZS 4214 method, and (ii) a modified method developed in this study and calibrated using the CFD results.

To produce updated DTS mitigation measures that align more closely with the CFD results, the modified thermal bridge calculation method developed previously for the ABCB [1] was adopted again in this project, with one important change. Rather than assigning a constant value to the pseudo air-layer R-value (R_{pa}) used in the method, it was assumed to vary with the batt thickness, and between the different types of ceilings (timber-framed, steel-framed, steel-framed with strips of insulation, and steel-framed with continuous insulation).

Figure 9 presents the models developed to give R_{pa} for each type of ceiling, and Figure 8 illustrates the accuracy of the modified method, in comparison with the standard NZS 4214 calculation method.

When the standard NZS 4214 method is applied to ceiling assemblies without including the adjacent roof space in the calculation, factors such as the following are neglected:

- Temperature differences between the exposed surfaces of frame members and batts on the top ceiling surface;
- Differences in emissivity between the exposed surfaces of frame members and batts on the top ceiling surface;
- Shielding and/or encapsulation of the top of frame members by the adjacent batts; and

- Protrusion of frame members above the batts (in cases with relatively thin batts);

The modified method used here corrects for such simplifications using a single empirical coefficient, R_{pa}. This is achieved using relatively simple models that have been calibrated to the limited set of CFD results shown in Figure 9. As such, this new method may not provide accurate results if it is applied to ceiling assemblies with significantly different construction details than those investigated here.
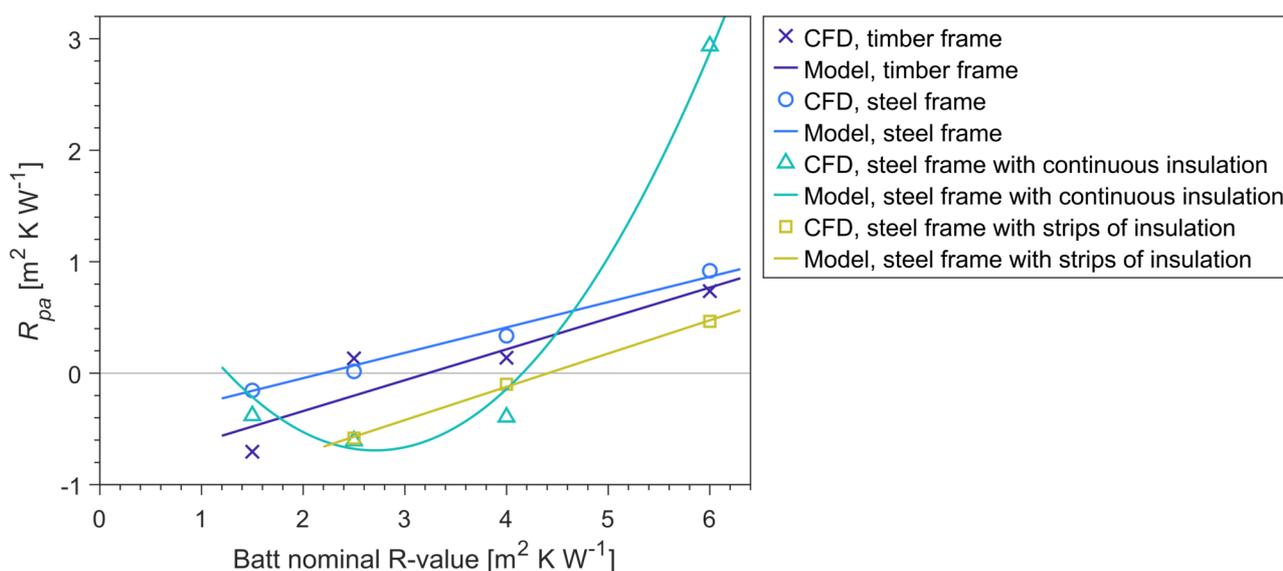

Figure 9: Models used to determine the pseudo air-space R-value, R_{pa}, which is used in the modified thermal bridge calculation method for ceilings. Results obtained using the method are shown in Figure 8.

Stage 2 of this project will focus on developing a more generally applicable thermal bridge calculation method for these types of assemblies. As part of this process, the interrelated impacts of factors such as those listed above will need to be disaggregated.

2.4.3 Updated DTS Mitigation Measures

Table 6 presents an updated version of Tables 13.2.3v and J3D7v from the NCC 2022 draft, including minimum thermal bridge mitigation measures needed to bring the 'typical' steel-framed ceilings investigated here to within either 95 % or 90 % (as outlined in Section 2.1) of the thermal resistance of an equivalent timber-framed ceiling.

Notably, no thermal bridge mitigation is required when the ceiling batt nominal R-value is 3 m^2 K W^{-1} or greater, and when mitigation is required, a relatively small amount of additional insulation would be sufficient.

Table 6: Updated minimum mitigation measures for Tables 13.2.3v and J3D7v of NCC 2022. These values represent the minimum level of mitigation needed to bring archetypal steel-framed ceilings to within either 95% or 90% of the R-value of corresponding archetypal timber-framed ceilings, as described in Section 2.1. Further rounding of these values may be appropriate. Moreover, it may not be reasonable to require NCC practitioners to install such small amounts of additional insulation (e.g. R0.06 insulation is likely to be 1.5–3 mm thick), so the ABCB may prefer omit requirements for thermal bridge mitigation for horizontal ceilings under pitched roofs in NCC 2022.

Minimum R-value from Tables 13.2.3a to 13.2.3i, and Table 13.2.3s if applicable	Option 1 - Increase insulation between ceiling framing to specified minimum R-value	Option 2 - Add insulation strips with specified minimum R-value above or below the ceiling framing	Option 3 - Add a layer of continuous insulation with specified minimum R-value above or below the ceiling framing
1.5	1.64	0.45	0.06
2.0	2.07	0.40	0.03
2.5	2.52	0.32	0.01
3.0			
3.5			
4.0			
4.5		No mitigation required	
5.0			
5.5			
6.0			

The level of additional insulation required in some cases is likely to be impractical to implement. For example, the requirement for continuous insulation with R-value of 0.06, 0.03 or 0.01 m^2 K W^{-1} would typically amount to layers of insulation that are less than 3 mm thick. The requirement for ceiling batts with R-value of 2.07 or 2.52 m^2 K W^{-1} is also likely to be impractical in many circumstances, as ceiling batts are not available in such small increments of R-value.

The decision of whether or not to specify such minor mitigation measures in the NCC will depend on how strictly the 95 and 90 % thresholds need to be adhered to.

2.5 RECOMMENDATIONS

The following recommendations have been developed based on this investigation.

A. The CFD simulations presented here have demonstrated once again that the standard NZS 4214 thermal bridge calculation method should not be used to calculate the R-value of horizontal ceilings under pitched roofs when: (i) the roof space is not included in the calculation, and (ii) the thermal bridging is relatively severe (such as that caused by

unmitigated steel bridges). Our previous investigations have also demonstrated that alternative one-dimensional thermal bridge calculation methods used in other jurisdictions suffer from similar levels of inaccuracy when applied to such ceilings, so they do not offer a solution to this problem. We recommend that a modified calculation method like that developed here be used in such cases. In Stage 2 of this project we will develop a more generally applicable calculation method for this purpose.

B. The thermal bridge mitigation measures outlined in Table 6 represent the minimum level of mitigation needed to meet the targets specified by the ABCB (i.e. to bring steel-framed ceilings to within 95 or 90 % of timber-framed R-values, depending on the level of insulation). We recommend that the practicability of such minor mitigation measures be considered, and that, if appropriate, these mitigation measures are either omitted altogether from the NCC or updated to meet alternative performance targets.

C. We recommend that, if the option to mitigate thermal bridges using strips of insulation installed over frame members is offered in the NCC, a requirement is included that the strips form a continuous layer of insulation with other insulation in the assembly. Otherwise, strips of insulation could be installed over frame members that protrude above ceiling batts (e.g. 90 mm frame members with R1.5 batts), leaving gaps in the thermal control layer and failing to mitigate thermal bridging effectively.

D. We recommend that the standard NZS 4214 be updated with a less ambiguous explanation of how the boundaries of thermally bridged layers should be defined, in line with the original work by Trethowen [3,4].

E. We recommend that further work be carried out to develop a generally applicable modified version of the NZS 4214 thermal bridge calculation method for application to building assemblies like the ceilings investigated here; and that the modified calculation method be included in NZS 4214. Without such a method being available to NCC practitioners, they are unable to accurately calculate the R-value of some types of building assemblies when attempting to meet minimum R-values specified in the NCC. Stage 2 of this project will build towards this goal.

F. We recommend that the treatment of thermal bridges in NatHERS software be reviewed, and that the methods be updated to address the issues demonstrated in this report if necessary.

3 Suspended Floors

The second investigation in this project was focused on thermal bridging in suspended floor assemblies. Such floors are typically insulated using batts or rigid foam boards installed between the floor joists, thus producing thermal bridges wherever joists penetrate the layer of insulation.

3.1 PROBLEM STATEMENT

As explained in Section 1, recent investigations have demonstrated that the NZS 4214 thermal bridge calculation method is inaccurate when applied to ceiling assemblies without including the roof space and roof in the calculation. It is likely that the same issue applies to suspended floor assemblies when their R-value is assessed separately from the subfloor space, subfloor walls and ground, as would be required under the draft NCC 2022 DTS Housing Provisions. When the NZS 4214 method is used to calculate the R-value of such floor assemblies without including the subfloor space in the calculation, the lower surface of floor joists and insulation are forced to the same temperature, producing unrealistic estimates of heat transfer through the joists and insulation.

The proposed NCC 2022 provisions for commercial buildings and apartments (in Volume 1) and the proposed Housing Provisions treat suspended floors differently:

- As described above, the Housing Provisions specify DTS insulation requirements and minimum R-values for suspended floor assemblies without including the thermal effects of the subfloor space (they are already accounted for by the precursor NatHERS simulations on which the DTS provisions are based); whereas
- Volume 1 specifies the minimum R-value of suspended floor systems including the subfloor space, and provides a set of nominal R-values for subfloor spaces (in Table S39C2a) that can be used in calculations.

Therefore, the accuracy/validity of the standard NZS 4214 calculation method could be different in these parts of the Code.

In this investigation, we have evaluated the accuracy of the standard NZS 4214 method when applied to suspended floors, as well as the accuracy of the nominal subfloor space R-values specified in Table S39C2a for a small number of cases. The aim of the investigation was to assess whether the types of issues identified for ceilings in Section 2 also apply to suspended floors.

3.2 METHODOLOGY

Two-dimensional, steady-state conjugate heat transfer CFD simulations were conducted to quantify the R-values of a set of suspended floor assemblies. The CFD methodology is very similar to that employed in our recent investigation into ceiling assemblies [1] and in Section 2 of this report, except it has been adapted to focus on suspended floors. Further details of the cases investigated are provided below, and Appendix A outlines the CFD settings and methods in more detail.

Results from the CFD simulations were compared to NZS 4214 isothermal planes calculations, and to the nominal R-values prescribed for subfloor spaces in Table S39C2a of the draft NCC 2022 Volume 1 provisions. Any discrepancies between the CFD and calculation results were analysed, and possible improvements to the calculation methods were proposed if appropriate.

3.3 CASES INVESTIGATED

3.3.1 Floor Assemblies

Table 7 outlines the set of floor assembly simulations that were run. Timber- and steel-framed cases were included with a range of insulation R-values, and with the insulation installed either flush with the top of the floor joists (labelled 'high' in Table 7) or flush with the bottom of the joists (labelled 'low' in Table 7) when the batt thickness is less than the joist height.

Figure 10a provides an example of the floor systems that were simulated. The subfloor space was assumed to be 600 mm deep in all cases, with an inlet vent on one wall and outlet vent on the opposite wall. The floor was modelled 8333 mm wide, to allow for an integer number of joists in both timber- and steel-framed cases. The subfloor walls were assumed to be formed by a single course of bricks, but were modelled as a thermal resistance within the simulation boundary conditions, rather than being resolved as solids within the computational domain. In all cases, the floor assembly was composed of 8 mm carpet, 10 mm underlay and 22 mm particleboard installed on top of the joists and insulation.

Two cases with R0.11 foil-faced foam wall wrap draped over the joists, instead of bulk insulation, were also simulated (Figure 10b), after the Energy Efficiency Technical Working Group indicated that this insulation arrangement is employed in some steel-framed suspended floors.

All timber- and steel-framed floors were simulated with a frame factor of 10.8 %, and contact resistances of 0.03 m^2 K W^{-1} were included wherever the joists and particleboard were in contact.

Table 7: Overview of suspended floor cases to be simulated.

| Case | Frame | | Insulation | | | Reflective facing[3] | Mitigation measure[3] |
	Material	Dimensions[1] [mm]	R-value [m² K W⁻¹]	Thickness [mm]	Position[2]		
1	steel	100×50×1.5	1	50	high	none	none
2	steel	100×50×1.5	1	50	low	none	none
3	steel	100×50×1.5	2	75	high	none	none
4	steel	100×50×1.5	2	75	low	none	none
5	steel	100×50×1.5	3	100	filled	none	none
6	steel	100×50×1.5	4	100	filled	none	none
7	steel	100×50×1.5	1	50	high	none	R0.26 continuous insulation under joists
8	steel	100×50×1.5	1	50	low	none	R0.26 continuous insulation under joists
9	steel	100×50×1.5	2	75	high	none	R0.51 continuous insulation under joists
10	steel	100×50×1.5	2	75	low	none	R0.51 continuous insulation under joists
11	steel	100×50×1.5	3	100	filled	none	R0.51 continuous insulation under joists
12	steel	100×50×1.5	4	100	filled	none	R0.51 continuous insulation under joists
13	steel	100×50×1.5	1	50	low	none	R0.51 strips under joists
14	steel	100×50×1.5	2	75	low	none	R0.64 strips under joists
15	steel	100×50×1.5	3	100	filled	none	R0.64 strips under joists
16	steel	100×50×1.5	4	100	filled	none	R0.64 strips under joists
17	timber	140×45	1	50	high	none	none
18	timber	140×45	1	50	low	none	none
19	timber	140×45	2	75	high	none	none
20	timber	140×45	2	75	low	none	none
21	timber	140×45	3	100	high	none	none
22	timber	140×45	3	100	low	none	none
23	timber	140×45	4	140	filled	none	none
24	steel	100×50×1.5	4	100	filled	insulation only	none
25	timber	140×45	4	140	filled	insulation only	none
26	steel	100×50×1.5	4	100	filled	frame and insulation	none
27	timber	140×45	4	140	filled	frame and insulation	none
28	steel	100×50×1.5	draped foil-faced foam wall wrap[5]			none	none
29	timber	140×45	draped foil-faced foam wall wrap[5]			none	none

[1] *Frame member dimensions are expressed as: height × width × base metal thickness (where relevant).*

[2] *Insulation position is either: high (i.e. flush with the top of the floor joists), low (i.e. flush with the bottom of the floor joists), or filled (i.e. the batt thickness is equal to the joist height, so they are flush at top and bottom).*

[3] *'Reflective facing' refers to a low-emittance (ε = 0.03) surface on the underside of the floor assembly, either covering the frame and insulation, or just the insulation.*

[4] *The R-value of additional insulation used for thermal bridge mitigation is based on proposed DTS provisions in the draft NCC Housing Provisions.*

[5] *Cases 28 and 29 include draped foil-faced foam wall wrap instead of bulk insulation.*
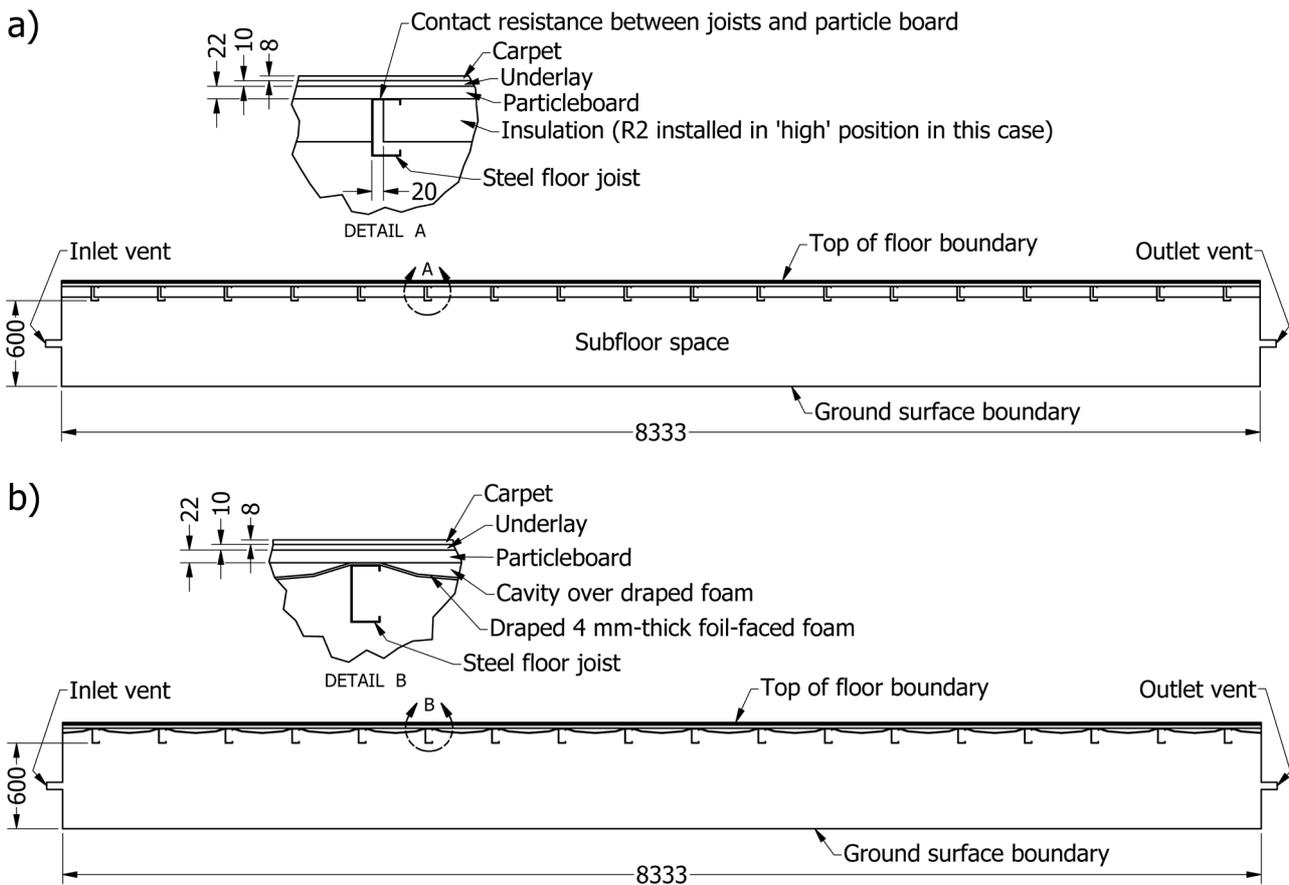
Figure 10: Computational domains used to simulate a suspended floor and subfloor spaces including (a) Case 3, with bulk insulation installed between joists; and (b) Case 27, with draped foil-faced foam insulation. All dimensions are expressed in mm.

3.3.2 Boundary Conditions

The boundary conditions applied to simulations of suspended floor systems are summarised in Table 8. The conditions were selected to represent a winter night, with standard indoor and outdoor 'film resistances' from AS 4859.2.

The effective thermal resistance of the ground was estimated using calculation methods outlined in CIBSE Guide A Section 3.5.5 [16], and using an assumed soil thermal conductivity of 1.2 W m^{-1} K^{-1}, taken from the AIRAH Technical Handbook [15].

The subfloor space ventilation rate was set in each simulation using a fixed velocity at the inlet vent and fixed pressure at the outlet. The ventilation rate was calculated using methods outlined in CIBSE Guide A Section 3.5.5 [16], and assuming the minimum ventilation opening size specified for Climatic Zone C in Volume 1 of the NCC (6,000 mm^2 per metre of subfloor wall length) and a reference wind speed of 2 m s^{-1}.

Table 8: Floor simulation boundary conditions.

Parameter	Value
Indoor temperature	18 °C
Indoor 'film resistance'	0.16 m^2 K W^{-1}
Outdoor air temperature	5 °C
Outdoor 'film resistance'	0.04 m^2 K W^{-1}
Brick subfloor wall thermal resistance	0.12 m^2 K W^{-1}
Ground effective thermal resistance	5.16 m^2 K W^{-1}
Subfloor space ventilation rate	0.119 L s^{-1} per m^2 floor area

3.3.3 Material Properties

The thermal properties of materials were primarily taken from the AIRAH Technical Handbook [15], and are summarised in Table 9. The thermal conductivity of underfloor insulation can vary significantly, depending on the material (e.g. whether it is rigid foam, mineral wool, or polyester), and the nominal thickness (underfloor insulation products with higher R-values tend to have lower thermal conductivity than those with lower R-values, so as to achieve the higher R-value without exceeding a thickness equal to the joist height). In this project, the thermal conductivity of the underfloor insulation was varied to achieve the insulation R-values and thicknesses in Table 7.

Table 9: Thermal material properties applied in simulations of suspended floors.

Material	Thermal conductivity [W m^{-1} K^{-1}]	Thermal emittance
Timber	0.12	0.9
Steel	47.5	0.23 or 0.28 [1]
Particleboard	0.108	0.9
Carpet underlay	0.505	0.9
Carpet	0.058	0.9
Underfloor bulk insulation	0.025–0.05 [2]	0.9 or 0.03 [3]
Continuous insulation and strips of insulation used for thermal bridge mitigation	0.035	0.9
Draped foil-faced foam	0.0364	0.03 (bottom), 0.1 (top) [4]

[1] *Based on a value of 0.23 for bright galvanized steel and increased by 0.05 for upward-facing surfaces to account for light dust cover* [15].

[2] *The thermal conductivity of underfloor insulation can vary relatively widely; the insulation thickness and R-value modelled in each case is presented in Table 7.*

[3] *Most cases simulated with non-reflective (i.e. ε = 0.9) insulation, but several simulated with a reflective facing; see Table 7.*

[4] *Based on values of 0.03 for downward-facing surface, and 0.05 with 0.05 increase to account for light dust cover on upward-facing surface.*

3.4 RESULTS

3.4.1 Floor Thermal Resistance

The R-values determined for each simulated floor assembly (measured between the top floor surface and bottom surfaces exposed to the subfloor space) are summarised in Table 10, and values from Cases 1–23 are compared to calculated R-values in Figure 11.

Table 10: R-values of suspended floors (not including 'film resistances') determined through the CFD simulations.

Case	Frame	Insulation	Bulk insulation position	Mitigation measure[1]	Floor R-value [m^2 K W^{-1}]	Ratio of floor R-value to that of corresponding timber-framed case [%]
1	steel	R1 batts	high	none	0.9290	72.64
2	steel	R1 batts	low	none	1.2297	80.68
3	steel	R2 batts	high	none	1.3301	64.02
4	steel	R2 batts	low	none	1.7002	73.92
5	steel	R3 batts	filled	none	2.0747	73.20 [2]
6	steel	R4 batts	filled	none	2.4128	66.46
7	steel	R1 batts	high	continuous	1.4544	113.72
8	steel	R1 batts	low	continuous	1.4775	96.94
9	steel	R2 batts	high	continuous	2.1874	105.28
10	steel	R2 batts	low	continuous	2.2639	98.43
11	steel	R3 batts	filled	continuous	2.6411	93.19 [2]
12	steel	R4 batts	filled	continuous	3.0233	83.27
13	steel	R1 batts	low	strips	1.3776	90.39
14	steel	R2 batts	low	strips	1.9887	86.46
15	steel	R3 batts	filled	strips	2.4145	85.19 [2]
16	steel	R4 batts	filled	strips	2.8574	78.70
17	timber	R1 batts	high	none	1.2789	100.00
18	timber	R1 batts	low	none	1.5241	100.00
19	timber	R2 batts	high	none	2.0776	100.00
20	timber	R2 batts	low	none	2.3001	100.00
21	timber	R3 batts	high	none	2.8342	100.00
22	timber	R3 batts	low	none	3.0252	100.00
23	timber	R4 batts	filled	none	3.6307	100.00
24	steel	R4 batts, reflective facing under batts only	filled	none	2.1940	63.01
25	timber	R4 batts, reflective facing under batts only	filled	none	3.4820	100.00
26	steel	R4 batts, reflective facing under batts and joists	filled	none	2.5390	69.16
27	timber	R4 batts, reflective facing under batts and joists	filled	none	3.6711	100.00
28	steel	draped R0.11 foil-faced foam	n/a	none	0.7078	74.92
29	timber	draped R0.11 foil-faced foam	n/a	none	0.9448	100.00

[1] *Mitigation measures include either continuous insulation or strips of insulation installed under the floor.*

[2] *Results from cases with steel frame and R3 batts have been compared to the timber-framed case with batts installed 'high' (i.e. Case 21).*

The R-values of steel-framed floors with unmitigated thermal bridges were found to equal 64–81 % of the corresponding timber-framed floor R-values. The mitigation of thermal bridging using a continuous layer of insulation underneath the floor was very effective in most cases, increasing the steel-framed floor R-value to 83–114 % of the corresponding timber-framed values. Strips of insulation installed underneath the joists proved to be less effective in the cases simulated, increasing the steel-framed floor R-values to only 79–90 % of the corresponding timber-framed values; strips of insulation with higher thermal resistance would need to be installed to achieve a greater effect.

Installation of the bulk floor insulation in a 'low' position (i.e. flush with the bottom surface of the floor joists) increased the R-values of timber-framed floors by 7–19 %, and steel-framed floors (without mitigation measures) by 27–32 %, as compared to cases where the insulation was installed in a 'high' position. These increases in effective R-value were caused by the formation of air-filled cavities above the insulation when it is installed 'low', and in cases with steel-framed floors, was also caused by the prevention of air exchange between the cavity inside each joist and the subfloor space.

The R-values of floors simulated with reflective (i.e. low-emittance) facing on the underside of the bulk insulation (i.e. Cases 24–27) were determined to be slightly lower than those of similar floors without such reflective facing. However, this does not indicate that the reflective facing degraded the thermal performance of the floors; in fact, it reduced the total rate of heat transfer through the floors by 18–41 %. The reason that this positive impact on thermal performance is not apparent in the floor R-values in Table 10 is that such effects are attributed to the subfloor space in our analysis, rather than to the floor assembly. While the reflective facing reduced the effective R-value of floors slightly, the thermal benefits provided by a reflective air space below the floor were much more significant than those changes in floor R-value. The impact of low-emittance surfaces on subfloor space R-values is discussed further in Section 3.4.3.

The timber- and steel-framed floors with draped foil-faced R0.11 foam insulation, rather than bulk insulation, were found to have effective R-values of 0.94 and 0.71 m^2 K W^{-1}, respectively. Two issues should be understood when interpreting these results, as outlined below.

1. Compression of the foam insulation between the floor joists and particleboard was not modelled in this study because we did not have sufficient data on the degree of compression that would occur or the thermal properties of the compressed foam. If such compression were modelled, the predicted R-value of the floors would be lower.

2. The R-values of these floors do not include the thermal benefits provided by the reflective facing on the underside of the foam insulation; those benefits are included in the sub-floor space R-values discussed in Section 3.4.3. This foil facing provided an additional thermal benefit of approximately 0.7–1.0 m^2 K W^{-1} in the cases investigated.

3.4.2 Accuracy of Calculation Methods

The standard NZS 4214 calculation method predicted floor R-values relatively accurately in cases with a timber frame or steel frame with continuous insulation installed as a thermal bridge mitigation measure (Figure 11). However, the R-values of steel-framed floors with unmitigated thermal bridges were severely underestimated by the NZS 4214 method in most cases, particularly when applied to floors with higher levels of insulation.
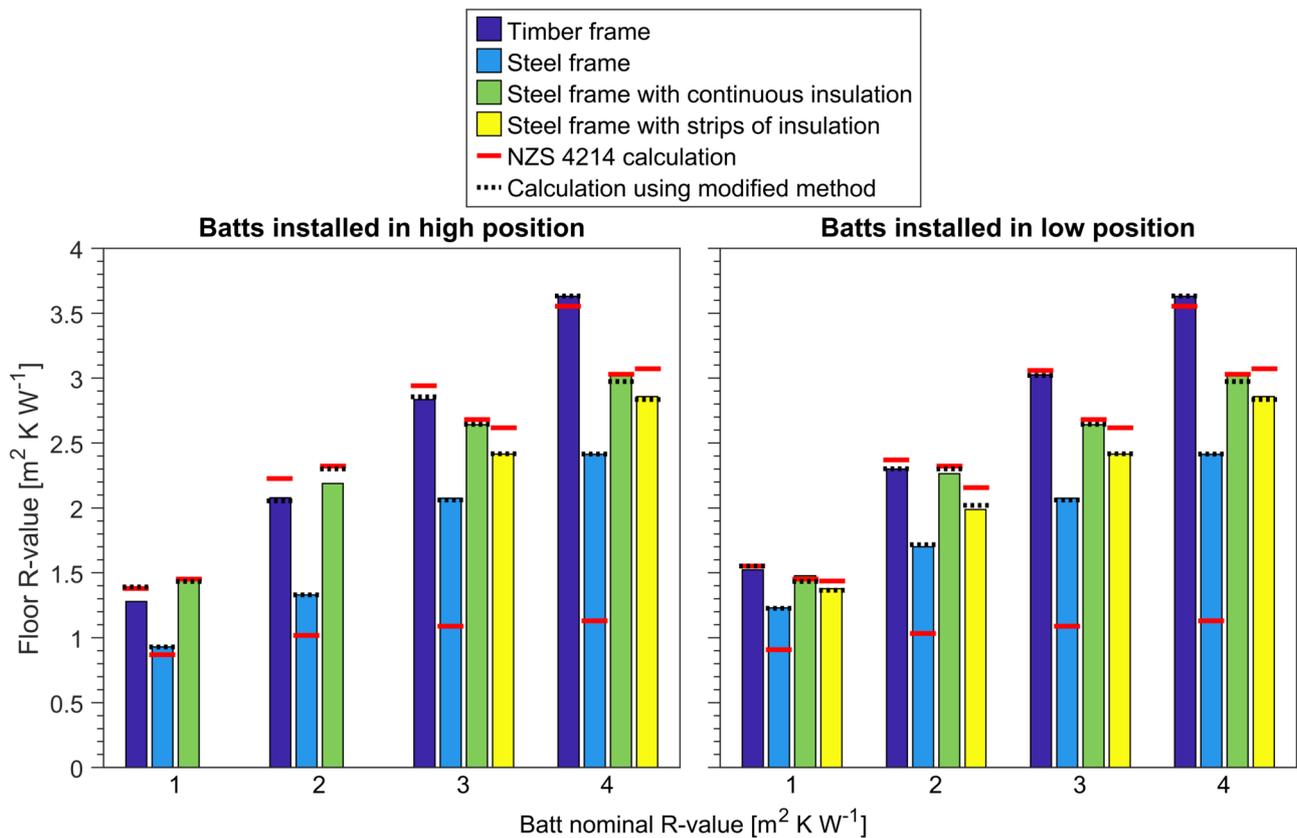

Figure 11: R-values of floor assemblies (not including 'film resistances') from CFD simulations of Cases 1–23, compared to standard NZS 4214 calculations and calculations using the modified method developed here. The left- and right-hand graphs display results from cases the bulk floor insulation is installed flush with the top and bottom surfaces of the floor joists, respectively. Results from cases where the bulk insulation height equals the joist height are included in both graphs.

This finding aligns closely with our observations from investigations into horizontal ceilings under pitched roofs (in previous studies [1,2], and in Section 2 of this report). When thermal bridges are

exposed on the surface of a building assembly (such as joists in suspended floors or in ceilings), and the thermal bridges are relatively severe (such as steel joists with no mitigation measures), the exposed surface of the thermal bridges can reach significantly different temperatures than the rest of the exposed surface of the building assembly. When the NZS 4214 calculation method is applied to such assemblies without including the air space adjacent to the exposed thermal bridges in the calculation, it can produce very inaccurate results.

By adopting the same approach applied to ceilings in Section 2.4, the R-values of suspended floors can be estimated much more accurately using a modified calculation method (as indicated by the dotted lines in Figure 11). The modified calculation method is identical to that developed in our previous project for the ABCB [1], except that the pseudo air-layer R-value (R_{pa}) is varied as a function of the floor assembly construction details. Figure 12 presents the models that were developed to give R_{pa}.
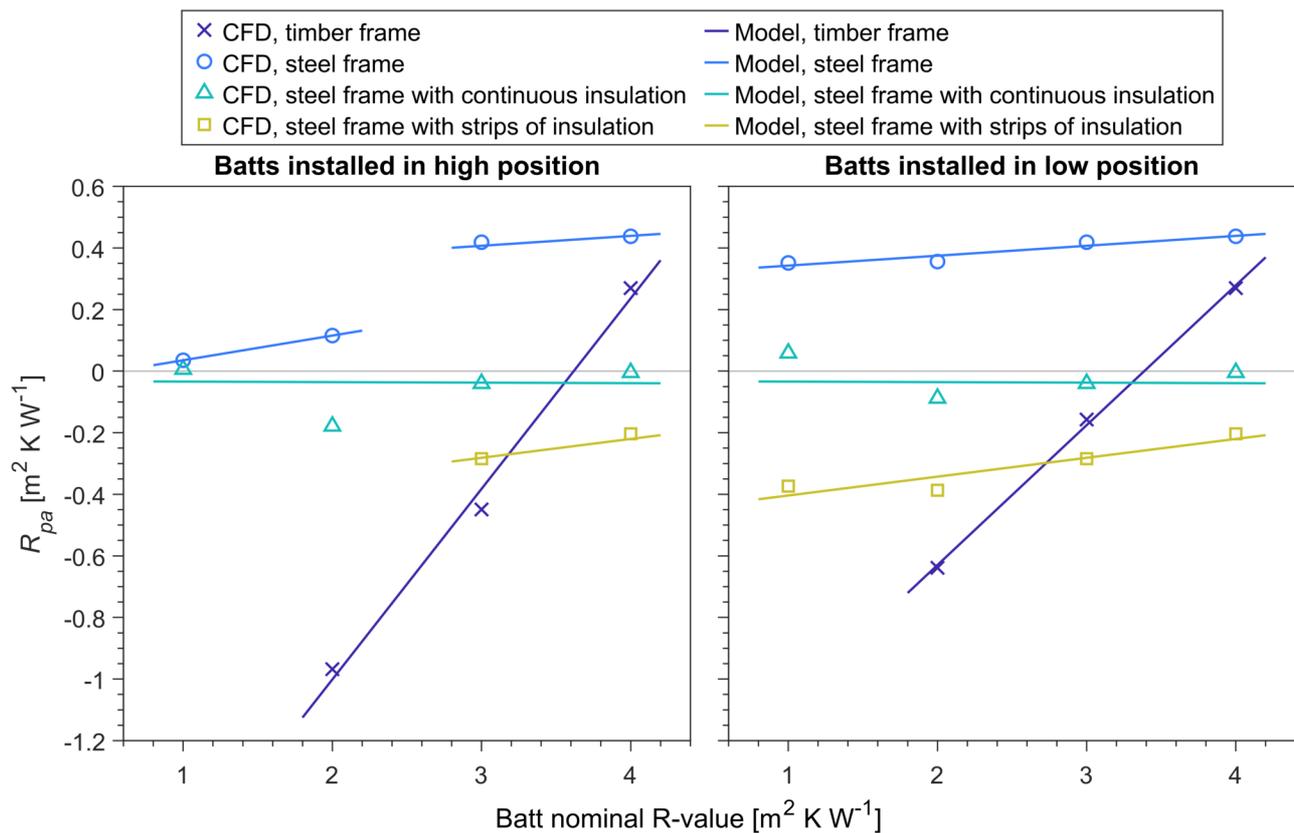

Figure 12: Models used to determine the pseudo air-space R-value, R_{pa}, which is used in the modified thermal bridge calculation method for suspended floors. Results obtained using these models are shown in Figure 11. Note that a separate model was developed for steel-framed floors that allow air exchange between the cavities inside each steel joist and the subfloor space (i.e. steel-framed floors with R1 or R2 insulation installed 'high' and no mitigation measures).

This modified calculation method is calibrated for the specific set of floor assemblies simulated in this study, and as such it would not necessarily be accurate if applied to floors with significantly different construction details (e.g. different frame member dimensions, frame factors, insulation arrangements, etc.). The method essentially corrects for several different sources of error using one calibrated parameter (R_{pa}), and the models developed to predict that parameter (shown in Figure 12) are not formulated in a way that takes each source of error into account individually. Therefore, the modified calculation method is not yet appropriate for general application to all types of suspended floor assemblies.

In Stage 2 of this project, we will aim to develop a more generally applicable calculation method for these types of thermally bridged assemblies.

3.4.3 Subfloor Space Thermal Resistance

The R-value of the subfloor space (i.e. the effective thermal resistance between the bottom surface of the suspended floor and the outdoor environment) was also calculated from each CFD result, for comparison with the nominal values in Table S39C2a of the draft NCC 2022. The source of the values in Table S39C2a does not appear to be cited in the NCC, but we believe they are likely to have been developed through one-dimensional thermal network calculations such as those described in CIBSE Guide A Section 3.5.5 [16] and ISO 13370.

Simulations of cases without a reflective facing on the underside of the suspended floor (i.e. Cases 1–23) predicted a relatively consistent subfloor space R-value, with an average value of 1.697 m^2 K W^{-1} and standard deviation of 0.056 m^2 K W^{-1}. Simulations of assemblies with reflective facing on the underside of the suspended floor produced significantly higher subfloor space R-values:

- 3.594 and 3.011 m^2 K W^{-1} for steel- and timber-framed cases, respectively, when the reflective facing covered the underside of floor batts but not joists (i.e. Cases 24 and 25);
- 4.675 and 4.693 m^2 K W^{-1} for steel- and timber-framed cases, respectively, when the reflective facing covered the undersides of floor batts and joists (i.e. Cases 26 and 27); and
- 2.739 and 2.399 m^2 K W^{-1} for steel- and timber-framed cases, respectively, when draped foil-faced foam was installed instead of bulk insulation (i.e. Cases 28 and 29).

In contrast, interpolation in Table S39C2a produces a value of 0.417 m^2 K W^{-1} for all of the subfloor spaces simulated—approximately one quarter of the value obtained through CFD for non-reflective

subfloor spaces, and between 7 and 11 times lower than the values obtained for reflective subfloor spaces.

AS 4859.2 [5] also includes a table of nominal subfloor space R-values, cites ISO 13370 as the methodology used to develop the table, and provides details of the assumptions made in the calculations. It specifies a value of 0.58 m^2 K W^{-1} for subfloor spaces similar to those simulated in this study, which is also significantly lower than the values determined from the CFD results.

The large discrepancies between Table S39C2a, AS 4859.2, and the CFD results presented here do not necessarily indicate that the table is invalid. Parameters such as the assumed thermal conductivity of soil can have a large impact on the predicted subfloor space R-value in both CFD and one-dimensional calculations, and different standards and codes recommend a wide variety of values for such parameters. For example, the NCC specifies a thermal conductivity of 0.6 W m^{-1} K^{-1} for soil, the AIRAH Technical Handbook specifies values ranging from 0.37 to 1.25 W m^{-1} K^{-1}, NZS 4214 specifies values ranging from 0.26 to 1.5 W m^{-1} K^{-1}, AS 4859.2 uses an assumed value of 1.5 W m^{-1} K^{-1}, and CIBSE Guide A specifies values from 1.5 to 3.5 m^{-1} K^{-1}. Moreover, the subfloor space R-value is sensitive to the assumed thermal resistance of the subfloor walls, subfloor space height, and subfloor ventilation rate.

Therefore, the following observations can be made regarding the subfloor space R-values in Table S39C2a.

- While Table S39C2a does not align with the CFD results presented here, it could be accurate for other subfloor spaces under certain conditions.
- The thermal resistance of real subfloor spaces is likely to vary significantly, depending on the local soil conditions, wind speed and direction, and subfloor construction. Tables of nominal R-values, such as Table S39C2a, would need to be very complex to capture all such variations accurately.
- However, Table S39C2a is relatively simplistic, and omits several important variables, such as the effects of surface emittance which can be very significant in some cases (increasing the subfloor space R-value from 1.697 m^2 K W^{-1} to values as high as 4.693 m^2 K W^{-1} in the cases simulated here), and the thermal resistance of subfloor walls.

3.5 RECOMMENDATIONS

The following recommendations have been developed based on this investigation (the letters used to identify each recommendation continue from the list of recommendations in Section 2.5).

G. When calculating the R-value of suspended floors separately from the subfloor space (as required under the draft NCC 2022 Housing Provisions), and the thermal bridging is severe (e.g. unmitigated metal frame members penetrating floor batts), the standard NZS 4214 calculation method should not be used. A modified calculation method can be applied to such floors. The method developed here produces accurate R-value estimates for suspended floors with the same construction details as those simulated here, and Stage 2 of this project is intended to produce a more generally applicable calculation method.

H. When calculating the R-value of suspended floors including the subfloor space (as required under the draft NCC 2022 Volume 1), the standard NZS 4214 calculation method is valid. However:

    c. The accuracy of the method in such cases will depend on the nominal R-value assigned to the subfloor space; and

    d. Instructions in NZS 4214 are currently ambiguous as to whether the subfloor space should be included in the 'bridged layer' in calculations.

    These issues are addressed in Recommendations I and D, respectively.

I. We recommend that, if Volume 1 of the NCC continues to require users to apply nominal R-values to subfloor spaces, those values (currently contained in Table S39C2a) be reviewed, and if appropriate updated to account for factors such as the thermal emittance of surfaces bounding the subfloor space, and the thermal resistance and height of subfloor walls. This review should also address inconsistencies between the subfloor space R-values specified in the NCC and those specified in Table 16 of AS 4859.2.

4 Flat, Skillion and Cathedral Roofs

Roof/ceiling assemblies in which the roof and ceiling planes are parallel, such as flat roofs, skillion roofs and pitched roofs with cathedral ceilings, exhibit different thermal behaviour to horizontal ceilings under pitched roofs, and are treated separately within the NCC. These roof types often feature thermal bridges where the roof purlins penetrate ceiling batts, and as such the accuracy of standard thermal resistance calculation methods when applied to flat/skillion/cathedral roofs should also be established.

4.1 PROBLEM STATEMENT

The primary issue that renders the standard NZS 4214 thermal bridge calculation method inaccurate for horizontal ceilings under pitched roofs is that, under the NCC, it needs to be applied to the ceiling assembly only, while the thermal performance of the roof and roof space are treated separately. This issue does not apply to flat, skillion and cathedral roofs under the proposed NCC 2022 provisions, since their R-values are specified/calculated for the entire roof/ceiling assembly. Material layers on the outdoor and indoor sides of the roof frame, and any insulation that it bridges, would confine the thermally bridged layer within NZS 4214 calculations. In this sense, flat/skillion/cathedral roofs are much like walls, for which the NZS 4214 method is relatively well validated [3].

However, another issue exists in the standard R-value calculation methods prescribed in the NCC that is likely to apply to flat/skillion/cathedral roofs. AS 4859.2 treats ventilated cavities using methods taken from ISO 6946 [11], by which they are classified as either 'unventilated', 'slightly ventilated' or 'well ventilated', depending on the size of openings that could allow ventilation. The thermal resistance of well-ventilated cavities, and any other material layers or cavities located on one side of the well-ventilated cavity, is then disregarded in calculations. Cavities classified as 'slightly ventilated' are addressed through linear interpolation between the 'unventilated' and 'well ventilated' R-values.

While this approach may be valid in situations where the assembly is exposed to a single indoor and single outdoor temperature, it does not account for the thermal benefits that cavity ventilation can provide when building assemblies are subjected to significant radiant heat transfer (e.g. solar heating, or radiant cooling at night). A previous project completed by the SBRC explored this issue in the
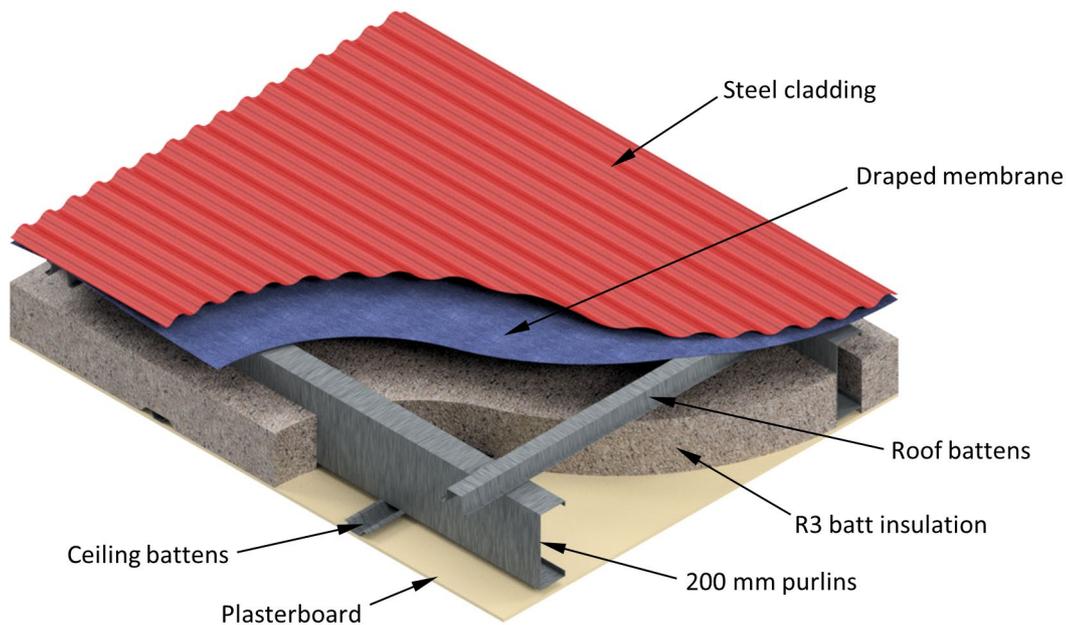
context of walls, and demonstrated that under many conditions the effective R-value of walls is actually increased by cavity ventilation, not decreased as predicted by AS 4859.2 [17].

Other research teams have also demonstrated the thermal benefits that ventilated cavities can provide in walls [18–20], predicting an increase in R-value of 15–60 % in the cases investigated. However, the majority of previous research into ventilated cavities has focused on the hygrothermal benefits that ventilation can provide.

This investigation was undertaken to assess the magnitude of error that the treatment of ventilated cavities in AS 4859.2 could introduce into R-value calculations for flat/skillion/cathedral roofs.

4.2 ANALYSIS

To demonstrate the magnitude of error that R-value calculation methods specified in AS 4859.2 can introduce when applied to flat, skillion and cathedral roofs, the skillion roof design shown in Figure 13 was analysed.

Figure 13: Partial cut-away diagram showing a section of the skillion roof design that was analysed.

The roof features:

- Steel cladding with solar absorptance of 0.6 and thermal emittance of 0.85;
- A pliable membrane with top surface emittance of 0.9 and bottom surface emittance of 0.03;

- Steel roof battens (40 mm × 43 mm effective width × 0.55 mm base metal thickness) installed at 1200 mm centres;

- Cold-formed steel 'C' purlins (200 mm × 76 mm × 1.5 mm base metal thickness) installed at 900 mm centres, with 144 mm-thick R3 glass wool batts installed between the purlins;

- Steel ceiling battens (20 mm × 30 mm effective width × 0.42 mm base metal thickness) installed at 600 mm centres; and

- A 10 mm-thick plasterboard ceiling lining.

The cavity formed between the membrane and batts in such a roof would typically be ventilated to some degree by air flow through openings formed (intentionally or inadvertently) around flashings at the edges of the roof. These openings could vary in size, from approximately 1 mm if the roof is designed to be airtight, through to tens of millimetres if openings near gutters and flashings are left open.

Applying the calculation methods specified in AS 4859.2 to the skillion roof, we obtain the estimated R-values in Table 11. Note that if the roof cavity is classified as 'well ventilated', the total R-value is predicted to decrease (by 25 or 41 %, depending on the direction of heat flow).

Table 11: R-values calculated for the skillion roof following procedures specified in AS 4859.2. The thermal resistance of the steel cladding and membrane are assumed to be negligible.

Material layer	R-value [m^2 K W^{-1}]			
	'Unventilated' cavity[1]		'Well ventilated' cavity[1]	
	Heat flow upwards	Heat flow downwards	Heat flow upwards	Heat flow downwards
Indoor 'film resistance'	0.11	0.16	0.11	0.16
Plasterboard	0.0588	0.0588	0.0588	0.0588
Purlins, batts, battens, and air spaces below and above membrane[2]	3.0590	4.1900	2.1560	2.2586
Outdoor 'film resistance'	0.04	0.04	0.11	0.16
Total	3.2678	4.4488	2.4349	2.6374

[1] *Under AS 4859.2, roof cavities are categorised as 'unventilated' when the total area of openings to is less than or equal to 500 mm^2 per square metre of roof area, and as 'well ventilated' when the total area of openings to is greater than or equal to 1500 mm^2 per square metre of roof area. For roofs with 'slightly ventilated' cavities, users of AS 4859.2 are directed to interpolate between values obtained for 'unventilated' and 'well-ventilated' cases.*

[2] *Thermally bridged layer includes 6 separate heat transfer paths and includes all materials and cavities between the plasterboard and steel cladding.*

To analyse the potential inaccuracy of AS 4859.2-derived R-values in Table 11, a thermal network model was developed to calculate steady-state heat transfer through the skillion roof. The model is based on the same type of one-dimensional formulation of thermal resistances that AS 4859.2 and NZS 4214 prescribe, but it allows the effects of ventilation to be modelled much more accurately as heat sources/sinks, and can model convective and radiant heat transfer separately, rather than assigning cavities an 'equivalent' R-value and external surfaces a 'film resistance'.

The rate of cavity ventilation was calculated using a flow network model, which balances the driving pressure due to wind and buoyancy with the aerodynamic resistance posed by narrow slot openings at the roof perimeter. For this exercise, it was assumed that the roof has an area 150 m^2, perimeter of 50 m, and height differential of 1 m between its higher and lower edge, and a single slot opening with gap width x around its perimeter.

Two sets of boundary conditions were modelled, including:

- Summer day, with an indoor temperature of 21 °C, outdoor air temperature of 30 °C, sky radiant temperature of 0 °C, solar heat flux incident on the roof of 250, 500 or 1000 W m^{-2}, and wind speed of 3 m s^{-1}.
- Winter night, with an indoor temperature of 21 °C, outdoor air temperature of 5 °C, sky radiant temperature of 5, –5 or –15 °C, no solar heat flux, and wind speed of 3 m s^{-1}.

Figure 14 compares the effective R-value of the skillion roof predicted using our model with values obtained using AS 4859.2, for a range of different ventilation opening sizes (x). Clearly the decrease in R-value predicted by AS 4859.2 when the roof ventilation openings become larger is not supported by the model in these cases. When the outdoor radiant load is relatively weak (e.g. when the solar heat flux is 250 W m^{-2} in summer, and when the sky temperature is similar to the outdoor air temperature in winter), cavity ventilation does reduce the effective R-value of the roof, but not nearly as much as is predicted by AS 4859.2. Moreover, when outdoor radiant heat transfer becomes more significant (e.g. in cases with higher solar heat fluxes, or larger differences between the sky and outdoor air temperatures), cavity ventilation can *increase* the effective roof R-value. Such thermal benefits can be substantial (in the order of several m^2 K W^{-1}) when the roof is subjected to strong solar heating.

These comparisons demonstrate the magnitude of error that can be introduced when cavity ventilation is modelled according to AS 4859.2 under a range of steady-state conditions. However, heat transfer

in buildings is dynamic, and the effects of cavity ventilation can vary significantly as conditions change.
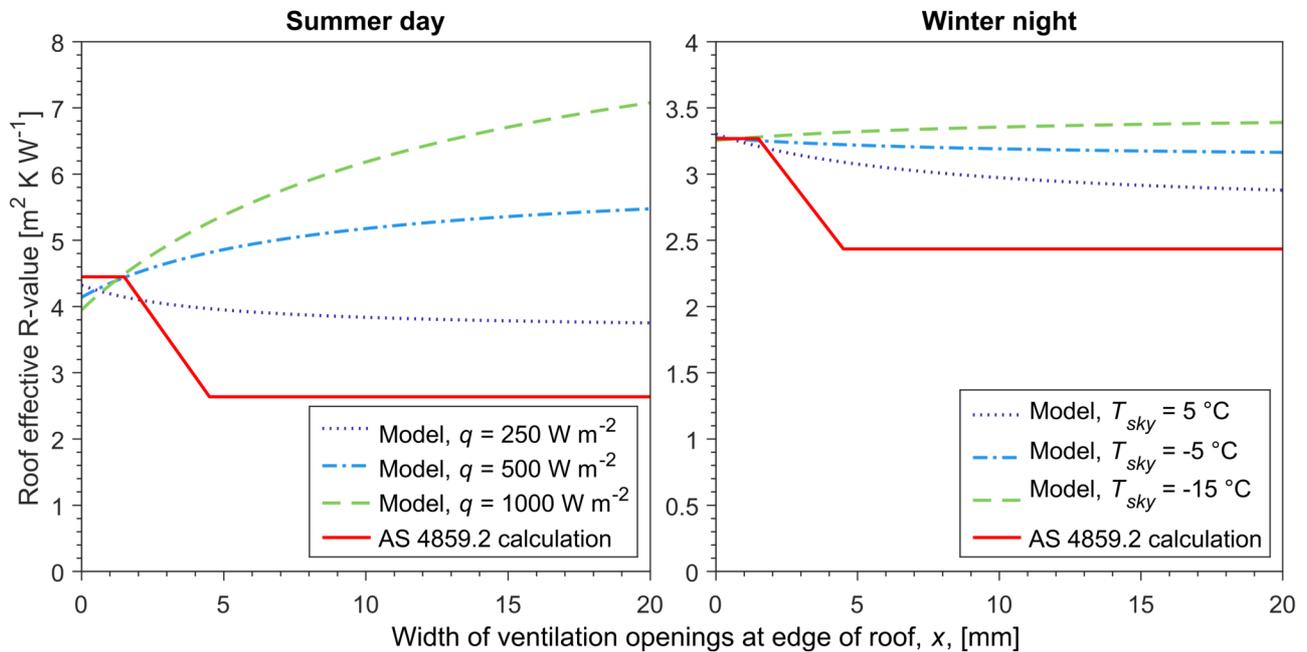

Figure 14: Comparison of skillion roof R-values determined using a thermal network model against the values calculated according to AS 4859.2. Results are presented over a range of ventilation opening sizes (x), and under several different steady-state conditions, including: (left) summer days with solar various solar heat fluxes (q) incident on the roof top surface; and (right) winter nights with various sky radiant temperatures (T_{sky}). Note that the two graphs have different vertical scales.

Ideally, R-values determined using standards such as AS 4859.2 should represent the effective thermal resistance of building assemblies, taken as some kind of average over an operational year. Thus, while the instantaneous effective R-value of the assembly may not match the calculated value under all conditions, the net impact of the assembly on annual energy consumption can be estimated relatively accurately. However, the current treatment of ventilated cavities in AS 4859.2 does not appear to do this, and is likely to underestimate the effective R-value of building assemblies with such cavities, such as typical flat/skillion/cathedral roofs.

4.3 RECOMMENDATIONS

The following recommendations have been developed based on this investigation (the letters used to identify each recommendation continue from the list of recommendations in Section 3.5).

J. The issues that arise when applying the NZS 4214 thermal bridge calculation method to ceilings or suspended floors and not including the adjacent air space in the calculation

(discussed in Sections 2 and 3), do not necessarily apply to typical flat/skillion/cathedral roofs. However, if cavities in the roof are classified as 'slightly' or 'well' ventilated under AS 4859.2, NCC practitioners are forced to calculate the roof R-value omitting that cavity and any other material layers on one side of it. This can give rise to situations where thermal bridges are exposed to an air space that is omitted from the calculation, in which case a modified version of NZS 4214 is likely to be needed. We recommend that the treatment of ventilated cavities in AS 4859.2 be reviewed and improved (see also Recommendation K, which is related).

K. The treatment of ventilated cavities in AS 4859.2 is likely to introduce significant errors in R-value calculations for flat/skillion/cathedral roofs that qualify as 'slightly' or 'well' ventilated under the standard. We recommend that the methods prescribed for ventilated cavities in AS 4859.2 be revised to more accurately represent the accumulated annual impact of such cavities when exposed to realistic boundary conditions (including separate outdoor radiant and convective heat transfer).

5 Conclusion

This project has focused on R-value calculation methods specified in the NCC (indirectly, through standards AS 4859.2 and NZS 4214) for:

- Horizontal ceilings under pitched roofs;
- Suspended floors; and
- Flat, skillion and cathedral-style roofs (with parallel ceiling and roof planes).

Using conjugate heat transfer CFD simulations and semi-analytical thermal network models, the accuracy of standard calculation methods has been evaluated for each of these applications.

Three key sources of inaccuracy have been identified:

1. Typically, when the R-value of an assembly is calculated without including an adjacent air space in the calculation, and relatively severe thermal bridges (e.g. metal frame members) are exposed to that air space, the standard NZS 4214 isothermal planes calculation method is not accurate.

2. The treatment of ventilated cavities in AS 4859.2 does not account for the thermal benefits that cavity ventilation can provide when building assemblies are exposed to realistic boundary conditions (e.g. when exposed to significant solar heat flux, or radiant cooling).

3. Nominal R-values assigned to subfloor spaces in the NCC (Table S39C2a) and other related documents (e.g. Table 16 in AS 4859.2) do not account for the effects of thermal emittance, subfloor wall thermal resistance, subfloor wall height, etc.

To address these issues, we have made 11 recommendations (labelled A–K) in this report, and Stage 2 of this project will make further progress on several of these fronts.

Ultimately, projects such as this will help to address inaccuracies in the NCC and associated standards, thereby improving effectiveness of efforts to:

- Decarbonise the Australian built environment; and
- Improve health and comfort conditions in Australian buildings.

References

[1]   A. Green, L. Kempton, P. Cooper, G. Kokogiannakis, Thermal Bridging of Horizontal Ceilings under Pitched Roofs, 2021.

[2]   A. Green, S. Beltrame, P. Cooper, Thermal bridging by ceiling frame members, 2021.

[3]   H.A. Trethowen, Validating the Isothermal Planes Method for R-Value Predictions, ASHRAE Transactions. 101 (1995) 755–766.

[4]   H.A. Trethowen, How are U on your R's?, in: IRHACE Conference, Napier, New Zealand, 1997.

[5]   Standards Australia, AS/NZS 4859.2:2018 Thermal insulation materials for buildings, Part 2: Design, (2018).

[6]   Standards New Zealand, NZS 4214:2006 Methods of Determining the Total Thermal Resistance of Parts of Buildings, (2006).

[7]   D. Chen, M. Ambrose, Thermal Bridging for Residential Building Energy Rating - Updated with NZS 4214, 2020.

[8]   T. Isaacs, Thermal Performance DTS Elemental Provisions for NCC 2022 - Draft Report, Brunswick, Victoria, 2021.

[9]   L. Kempton, G. Kokogiannakis, A. Green, P. Cooper, Evaluation of thermal bridging mitigation techniques and impact of calculation methods for lightweight steel frame external wall systems, Journal of Building Engineering. 43 (2021) 102893. https://doi.org/10.1016/j.jobe.2021.102893.

[10]   E. Kenna, L. Boland, Thermal Bridging - Calculations and Impacts, in: AIRAH and IBPSA's Australasian Building Simulation Conference, Melbourne, Australia, 2017.

[11]   International Organization for Standardization, ISO 6946 Building components and building elements - Thermal resistance and thermal transmittance - Calculation methods, (2017).

[12]   M. Gorgolewski, Developing a simplified method of calculating U-values in light steel framing, Building and Environment. 42 (2007) 230–236. https://doi.org/https://doi.org/10.1016/j.buildenv.2006.07.001.

[13] S.M. Doran, M.T. Gorgolewski, BRE Digest 465: U-values for light steel-frame construction, Building Research Establishment, Watford, UK, 2002.

[14] ASHRAE, Handbook: Fundamentals, The American Society of Heating, Refrigerating and Air-Conditioning Engineers, Atlanta, GA, USA, 2017.

[15] AIRAH, Technical Handbook, 5th ed., The Australian Institute of Refrigeration, Air Conditioning and Heating, Melbourne, Australia, 2013.

[16] Chartered Institution of Building Services Engineers, CIBSE Guide A - Environmental Design, 8th ed., London, 2015.

[17] A. Green, P. Cooper, Hygrothermal performance of metal wall cladding systems, Wollongong, Australia, 2020.

[18] R.W. Guy, T. Stathopoulus, Mechanisms of Pressure Differences Across Building Facades, in: First Annual Conference on Building Science, The Canadian Society for Civil Engineering, London, Ontario, 1982.

[19] M. Ciampi, F. Leccese, G. Tuoni, Ventilated facades energy performance in summer cooling of buildings, Solar Energy. 75 (2003) 491–502. https://doi.org/10.1016/j.solener.2003.09.010.

[20] C. Marinosci, G. Semprini, G.L. Morini, Experimental analysis of the summer thermal performances of a naturally ventilated rainscreen façade building, Energy and Buildings. 72 (2014) 280–287. https://doi.org/10.1016/j.enbuild.2013.12.044.

Appendices

APPENDIX A: CFD METHODOLOGY

The CFD simulations described in this report were based on a finite-volume formulation of the Reynolds-averaged Navier Stokes (RANS) equations. The shear stress transport (SST) $k\text{-}\omega$ turbulence model was used, with low-Reynolds number treatment near walls (the mesh was kept fine enough near walls to maintain a dimensionless near-wall distance, y^+, less than one). In cases involving small, restricted air spaces, laminar flow was simulated in those small air spaces.

Buoyancy effects were simulated using the Boussinesq approximation. Radiant heat transfer between surfaces bounding the roof space was simulated using the discrete ordinates model, and by treating all surfaces as opaque, grey and diffuse.

The simulations were run using the coupled pressure-based solver in ANSYS Fluent, and adopting the PRESTO! scheme for spatial discretisation of pressure and second-order upwind discretisation for all other field variables.